Microchimica Acta (2018) 185: 283
https://doi.org/10.1007/s00604-018-2809-3

REVIEW ARTICLE

Electrodes modified with 3D graphene composites: a review on methods for preparation, properties and sensing applications

Nadeem Baig [1] · Tawfik A. Saleh [1]

Received: 4 February 2018 / Accepted: 14 April 2018 / Published online: 7 May 2018

Abstract

Three-dimensional (3D) porous networks of planar 2D graphene have attractive features with respect to sensing. These include a large electroactive surface area, good inner and outer surface contact with the analyte, ease of loading with (bio)catalysts, and good electrochemical sensitivity. 3D free-standing graphene can even be used directly as an electrode. This review (with 140 refs.) covers the progress made in the past years. Following an introduction into the field (including definitions), a large section is presented that covers methods for the synthesis of 3D graphene (3DG) (including chemical vapor deposition, hydrothermal methods, lithography, support assisted synthesis and chemical deposition, and direct electrochemical methods). The next section covers the key features of 3DG and its composites for use in electrochemical sensors. This section is subdivided into sections on the uses of 3D porous graphene, 3DG composites with metals and metal oxides, composites consisting of 3DG and organic polymers, and electrodes modified with 3DG, 3DGs decorated with carbon nanotubes, and others. The review concludes with a discussion of future perspectives and current challenges.

Keywords Porous carbon · Three-dimensional material · Quantum dots · Lithography · Hydrothermal synthesis · Chemical vapor deposition · 3D printing · Electrochemical sensor · Biosensor · Conductive polymer · Nanoparticles

Introduction

Graphene consists of a single layer of sp^2 hybridized carbon atoms arranged in a honeycomb-like lattice [1]. Graphene has made its way into different fields of research including photocatalysis, batteries, electrochemical sensors and biosensors, gas sensors, and supercapacitors [2, 3]. Graphene is an interesting two-dimensional (2D) planar material which can be rolled into one-dimensional (1D) nanotubes, wrapped into zero-dimensional (0D) fullerenes. The sheets stacking result in the formation of three-dimensional (3D) graphite [1, 4]. Graphene displays amazing exceptional characteristics. It is the known thinnest material in the universe and the strongest ever measured material [5]. It is transparent with incredible flexibility [6]. Its optical transparency is ~97.3% [7, 8]. Graphene mechanical strength is 200 times superior to steel [9]. Graphene has an exceptionally high theoretical surface area (2630 $m^2\ g^{-1}$) which is substantially huge compared to graphite (~10 $m^2\ g^{-1}$) and two times larger than the carbon nanotubes (1315 $m^2\ g^{-1}$) [10]. Graphene displayed the ultra-high electron mobility 200,000 $cm^2\ V^{-1}\ s^{-1}$ with charge density ~2×10^{11} cm^{-2} [10–12]. Graphene possessed extraordinary thermal conductivity of 3000 WmK^{-1} [13, 14]. It is obvious that electrode materials perform a critical role in the fabrication of high-performance electrochemical sensor [15]. These unique and extraordinary physicochemical properties solidify the role of graphene in the field of material science and forthcoming technology.

Materials that are closely related to graphene are sometimes referred to as graphene. In some applications, both graphene oxide (GO) and reduced graphene oxide (rGO) also have been denoted as graphene. However, the pristine graphene has some obvious differences from GO and rGO. Graphene is a 2D material which only contains sp^2 hybridized carbon atoms, whereas GO is a monolayer of graphite oxide. GO contains both sp^2 and sp^3 carbon atoms. The sp^3 bonding in GO is around 40% [16]. It also has many oxygen-containing functional groups. The hydroxy and the epoxy groups are present on the basal plane and the sheet edges of the GO contain phenol, quinone, lactone, carbonyl, and

✉ Nadeem Baig
nadeembaig@kfupm.edu.sa; nadeembaig38@gmail.com

[1] Chemistry Department, King Fahd University of Petroleum and Minerals, Dhahran 31261, Saudi Arabia

carboxy groups. These covalently attached oxygen-containing functional groups generate extensive structural defects in the GO sheet compared to pristine graphene. These functional groups severely affect its mechanical and electrochemical properties. The poor electrochemical behavior put a limitation on the direct use of GO as an electrode material [17]. Electrochemical behavior of the GO is improved by reducing the GO with the help of chemical or electrochemical methods [18]. During reduction, certain oxygen-containing functional groups are lost which improve the electrochemical activity of the rGO. The carrier mobility of the chemically rGO is substantially lower compared to pristine graphene [16]. The conductivity of the rGO is improved up to an order of 4 compared to GO. The conductivity of the reduced GO is far behind (around a factor of 10–100) from pristine graphene [19]. Since the properties of the rGO are substantially different from graphene, it is not appropriate to refer rGO as graphene strictly [20]. Graphene quantum dots (GQDs) are small graphene pieces with nanometer size [21]. In GQDs the properties of the graphene and the quantum dots are merged. The different graphene and graphene-related materials are appropriately defined in Table 1.

Graphene has proved a revolutionary outstanding electrode material due to its wide potential window, relatively inert behavior, and low cost. For electrochemical sensing, the graphene offered a wide potential window of 2.5 V in 0.1 M phosphate buffer (pH 7.0). Graphene has tremendous potential in the field of electrochemical sensing due to its exceptional electron transfer and the carrier mobility [28]. Moreover, it is lightweight, thermally and mechanically stable which made them an ideal material [29] for sensor fabrication. Modification of the electrode surfaces with graphene assists the electrode to achieve trace level quantification of the analytes with better reproducibility.

The intrinsic properties of graphene are severely compromised as the graphene nanosheets irreversibly agglomerate into a graphitic form. The restacking of the graphene nanosheets triggered from the basal plane of the graphene is due to the strong van der Waals forces and the π–interactions [30]. This agglomeration severely affects the intrinsic characteristics of graphene. As a result, the high surface area and exceptional conductivity of graphene is extensively compromised [31].

It is a challenge to preserve the intrinsic characteristics of graphene by inhibiting the restacking of graphene into graphitic form. The separation between the graphene sheets was tried to achieve by the incorporation of spacers [32] such as metals, metallic oxide, conductive polymers, carbon nanofiber (CNF) and carbon nanotubes (CNTs) [33–38]. The introduction of spacers somehow assists to separate the graphene layers. Researchers are constantly focusing on the new architectures of 2D graphene to achieve more refined results by overcoming the issue of restacking and agglomeration.

The 3D architecture of 2D graphene is an attempt to extend the successful utilization of the graphene. 3D porous materials with interconnected ordered structures are gaining technological importance in various applications. 3D architecture substantially improved the performance of the certain devices [39]. 3D graphene has several advantages to use it as an electrode material. The 3D graphene porous network for sensing applications provides a large surface area and facilitates the facile movement of electrolytes which allows the better contact of the analyte with the active sites of the sensing electrode. 3D graphene also acts as a scaffold for loading of other nonmaterial [40]. The 3D graphene provides a better opportunity for the loading of catalysts, enzymes, and nanomaterial to fabricate electrochemical sensors for selective and sensitive quantification of the analytes. 3D graphene continuous porous network prevents the aggregation of the metal nanoparticles or other functional materials which are loaded or embedded for certain sensing application. Different 3D materials including 3D macroporous Pt films, 3D Porous nickel nanostructures, 3D aperiodic hierarchical porous graphitic carbon, 3D CNT ensembles electrode, 3D CNF, nanodiamonds and 3D porous carbon were applied to the electrochemical applications [41–47]. This review is only focusing on 3D graphene-based electrochemical sensors.

The three-dimensional graphene design has a good future in many challenging applications such as catalyst support, stretchable conductors, environmental protection, biofuel cells, energy storage devices, gas sensors, and electrochemical sensors [48–58]. 3D graphene is a promising material for electrochemical sensing and proved an outstanding material for fabrication of electrochemical sensors [59]. The 3D porous network of graphene provides a platform to make different composites by using the porous network [60]. Expanding the 2D graphene into 3D architecture is a fascinating and further functionalization with other materials helps researchers to manipulate the material to any extent for desired results. The 3D graphene porous network is a promising electrode material due to light weight and excellent conductivity. There are only a few reviews on the 3D graphene porous network which mainly focus on synthesis and energy-related applications [8, 61–63]. There is no review written that specifically focuses on the application of 3D graphene porous networks for electrochemical sensing. There is a need to consolidate the work for future progress in the fabrication of 3D graphene electrodes.

Synthesis of three-dimensional graphene

Freestanding three-dimensional graphene or porous networks of graphene can be attained by various methods including template assembly and self-assembled graphene nanosheets [30]. The template strategy was commonly applied in several

Table 1 Definitions of graphene and graphene-related materials

Material	Definition	Ref.
Graphene (G)	It is a monolayer of a 2D planar sheet of carbon atoms packed in the honeycomb-like lattice.	[1]
3D Graphene (3D G)	3D graphene is the porous network of interconnected graphene sheets.	[22]
Graphene oxide (GO)	It is a single layer of the graphite oxide contains randomly distributed oxidized (sp^3) and non-oxidized zone (sp2). It contains the oxygen-containing functional groups such as epoxy, hydroxyl, carbonyl, quinone, lactone, and carboxyl. It has disrupted sp^2 bonding network due to these oxygen-containing functional groups.	[17, 23]
Reduced graphene oxide (rGO)	Reduced graphene oxide is a single layer of carbon atoms with some unwanted oxygen functional groups and it is attained by chemical or electrochemical reduction of graphene oxide. During reduction, many defects generated on the surface of rGO and it cannot restore the full properties of graphene. It is not perfectly sp^2 due to the presence of defects and residual oxygen functional groups.	[20, 24]
Carbon dots	Carbon dots term used for small nanoparticles of carbon which size is less than 10 nm	[25]
Graphene quantum dots (GQDs)	GQDs are the well-confined space 0D nanometer size pieces of monolayer graphene sheet. It contained unique properties of both quantum dots and graphene	[26]
Graphene oxide quantum dots (GOQDs)	GOQDs are the tiny pieces of single-layer graphene oxide which are several nanometers in size. Sometimes this terminology is also referred to few-layered graphene oxide	[27]

methods including chemical vapor deposition (CVD), solvothermal, sol-gel and hydrothermal synthesis to attain 3D porous graphene. Various templates such as Ni foam, Cu foam, polystyrene spheres, etc. were used for the fabrication of 3D graphene. The template-based synthesis of the 3D porous network generally consists of three steps. In the first step, the reaction precursors are attached to the template either by incorporation or impregnation. In the second step of the reaction, growth or nucleation is continued to form the solid species either in or on the template surface. In the last step, the template was removed by several ways to form a 3D porous structure [62]. A few methods based on a template or the templateless generation of 3D graphene is discussed.

Chemical vapor deposition

The chemical vapor deposition method is frequently applied for the synthesis of 3D graphene [64, 65]. The template-directed CVD method was used to synthesize the 3D foam consists of graphene macroscopic structure. In CVD method, the graphene is deposited on the 3D support by the decomposition of the various carbon-containing sources at high temperature. After deposition, the support is etched away chemically. Collapsing of graphene is prevented by depositing the thin layer of poly (methyl methacrylate) (PMMA) on the graphene film before etching process [66]. The 3D graphene network was generated on the nickel foam from the high-temperature decomposition of CH_4. The 3D scaffold of Ni is etched away with the help of HCl to achieve a 3D continuous graphene network. Prior to etching, the graphene films were protected by poly (methyl methacrylate) (PMMA). The polymer was later on removed by the acetone treatment [66]. Xiehong Cao et al. [67] also used the CVD method based on nickel template foam for the generation of 3D graphene networks. Later on, the 3D graphene was coated with MWCNTs, Pt NPs, and MnO_2 NPs to obtain various composites of 3D graphene. Similarly, 3D graphene was obtained to construct a monolithic free-standing electrochemical sensor [68]. The CVD method was used for in situ growth of cobalt oxide nanowires on the 3D graphene foam [31]. This approach facilitates the monolith fabrication of the 3D graphene network. In a continuous grown 3D graphene network, the charge carriers move more rapidly. CVD synthesized 3D graphene provides a high surface area on which various active materials can be anchored to impart specific characteristics for sensing applications. It also offers excellent conductive channels which allow the rapid electron transfer. CVD method also provides an opportunity to tune the pore size using metal-based nanotemplates which range from 50 nm to 1 μm [69]. The porous structure provides a platform for efficient contact between the electrode surface and the electrolyte [67]. The graphene network acquired from CVD displayed a good interconnection but poor mechanical stability. The mechanical issue arises

due to the soft framework of pristine graphene. The large-scale production of 3D graphene is challenging due to the consumption of the template which leads to high production costs [70].

Hydrothermal method

The hydrothermal strategy was also applied to obtain a 3D graphene or rGO hydrogel. The rGO hydrogel is synthesized by sealing the GO into the autoclave reactor for several hours at high temperature. The PdCu nanoparticle (NP) decorated 3D graphene hydrogel was obtained from the aqueous dispersion of ethylene glycol, GO, glutamate and the salts of palladium(II) and copper(II). In a stainless-steel autoclave, the dispersion was sealed for several hours of heating to obtain a metallic nanoparticle decorated 3D rGO hydrogel [71]. In another work, self-assembled rGO hydrogel was obtained from GO using a one-step hydrothermal process (Fig. 1). The hydrogel was achieved by sealing GO into a Teflon-lined autoclave for heating at 180 °C for 1–12 h [72]. Similarly, the nitrogen-doped rGO hydrogel was obtained by gradually adding organic amine or ammonia into the GO prior to subjecting it to hydrothermal treatment [73]. Hydrothermal methods are simple and the 3D rGO composite with other nanomaterial is synthesized easily by mixing them with GO. Morphology can be controlled by those methods in which template are involved. In templateless methods, control of morphology is difficult to achieve.

Lithographically defined three-dimensional graphene structures

Lithography has emerged as a powerful tool for attaining 3D architectures [74]. 3D carbon can be achieved in lithography using photoresist structures. The thin nickel film was sputtered uniformly on the lithographically-defined conductive three-dimensional carbon networks. Further annealing of the Ni-coated carbon resulted in the fabrication of the multilayer graphene-coated 3D Ni electrode [75]. The multilayer graphene hollow structure can form by removing the Ni through acid etching (Fig. 2). Overall three steps are required to convert the predefined 3D pyrolyzed photoresist films into 3D porous graphene. In the first step, the Ni was sputtered on the 3D amorphous carbon structure; while the second step consisted of annealing. In the last step, the Ni was removed by acid etching to give a multilayer graphene hollow structure (Fig. 3) [76]. One of the major advantages to using the porous network is the huge available surface area and availability of the interior surface for the electrochemical reaction. Sometimes, the nanopores high density and the wide size-

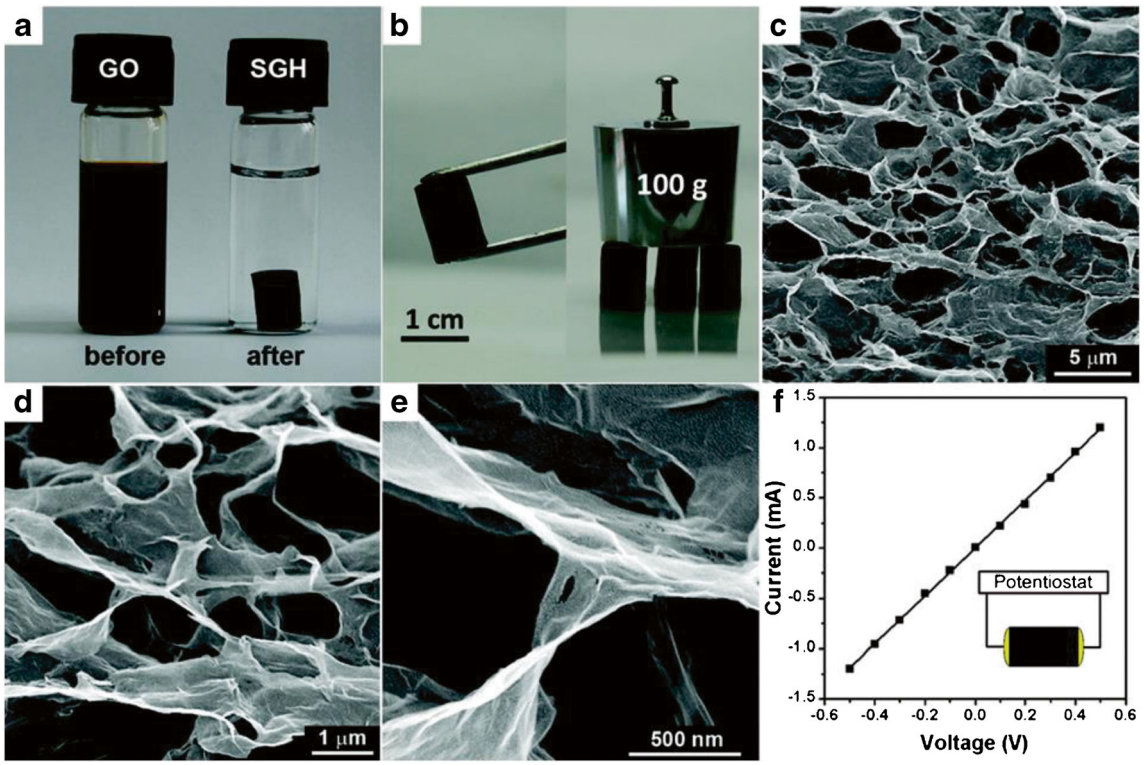

Fig. 1 **a** Photographs of a 2 mg/mL homogeneous GO aqueous dispersion before and after hydrothermal reduction at 180 °C for 12 h; **b** photographs of a strong SGH allowing easy handling and supporting weight; **c**–**e** SEM images with different magnifications of the SGH interior microstructures; **f** room temperature I–V curve of the SGH exhibiting Ohmic characteristic, inset shows the two-probe method for the conductivity measurements [72]. Copyright (2010) American Chemical Society

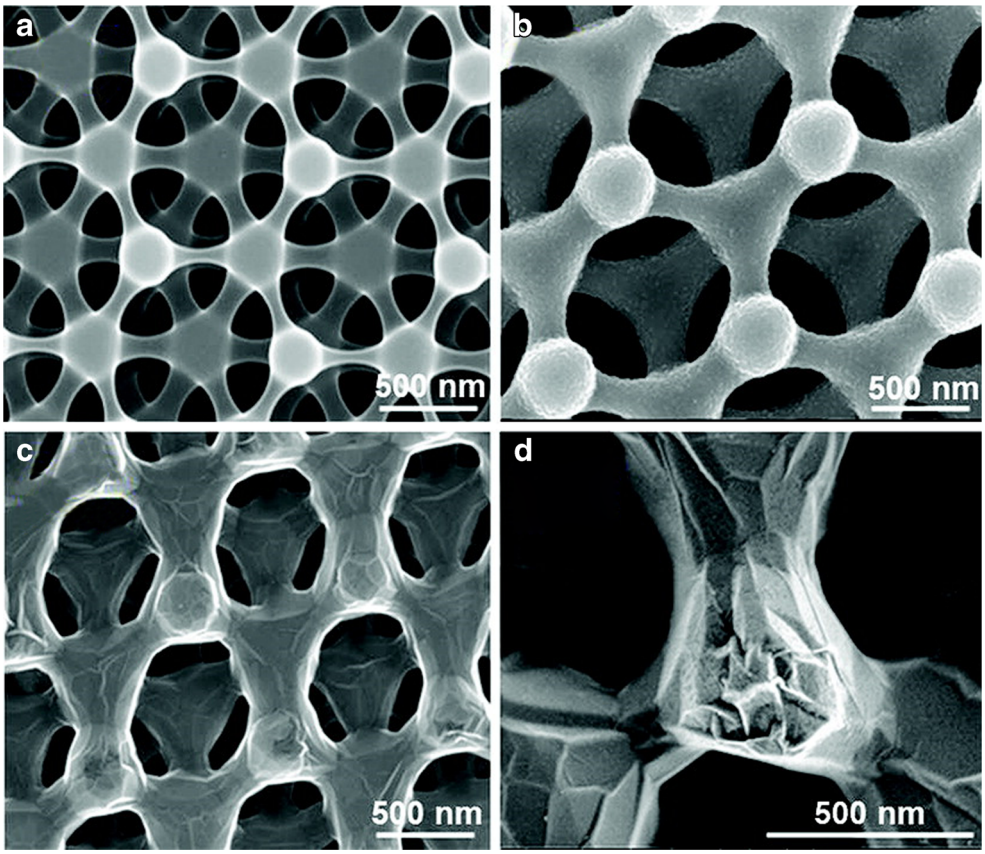

Fig. 2 SEM images of the lithographically generated porous carbon (**a**), porous carbon coated with nickel before thermal annealing (**b**), and 3D graphene structure after annealing at 750 C° and etching of Ni layer in a 2 M H_2SO_4 solution (**c**, **d**) [76]. Copyright (2012) American Chemical Society

distribution of the pores may lead to the overlapping diffusion regions which may limit the mass transport to the interior region of the porous network. The benefit of the high surface area does not remain much effective [75]. The highly ordered fabrication of the mesoporous material might be a possible solution. Lithography provided more controlled fabrication of 3D interconnected porous electrode. The controlled morphology provided several pathways for the analyte to diffuse and the electrochemical reaction takes place throughout the porous electrode surface. The nanofabrication through conventional lithography is a complex, expensive and time-consuming process [77].

Support assisted and chemically deposited three-dimensional graphene

Reduction of the GO is very common by using different reducing agents. GO is reduced with the help of a reducing agent on a 3D support to obtain a 3D network of rGO. Fei Liu et al. [78] fabricated a 3D rGO architecture using polydimethylsiloxane (PDMS) micropillars. The GO was adsorbed on the PDMS micropillar and reduced chemically with hydrazine vapors. Freeze drying is another method to obtain a 3D network. There are two main steps involved in synthesizing 3D rGO by the freeze-drying method. In the first step, the GO was reduced by using a reducing agent such as hydrazine hydrate. In the second step, the rGO was freeze-dried to obtain a 3D network [59]. Similarly, a 3D-AuNP/rGO composite was also synthesized by reducing the GO and the $HAuCl_4{\cdot}4H_2O$ using polyethylene glycol as a reducing agent. After reducing, it was freeze-dried [79]. Sacrificial templates were also used for the synthesis of 3D graphene. Polystyrene is the commonly used sacrificial template [80]. The graphene spheres were generated by mixing the positively charged polystyrene spheres into the negatively charged GO solution. Due to the electrostatic force of attraction; the negatively charged GO sheets wrapped around the polystyrene spheres to neutralize the charge. A high number of GO sheets are wrapped due to the π–interactions. The spherical shell wrapped GO sheets were reduced with hydrazine to achieve the PS@graphene core-shell structure. The polystyrene template was removed by heat treatment to obtain the graphene hollow spheres [81]. For the electrochemical sensor application, 3D rGO nanosheets were also fabricated using a polystyrene spheres template. After the reduction of GO, the template was removed by the toluene sonication [82].

Three-dimensional graphene-polyaniline hybrid hollow spheres (3D rGO-PANI HS) were also fabricated using polystyrene as a template. GO was reduced in the presence of polystyrene sulfonate. The sulfonated group imparts the negative charge to the rGO and provides a stable dispersion of negatively charged rGO. The positive charge PANI dispersion

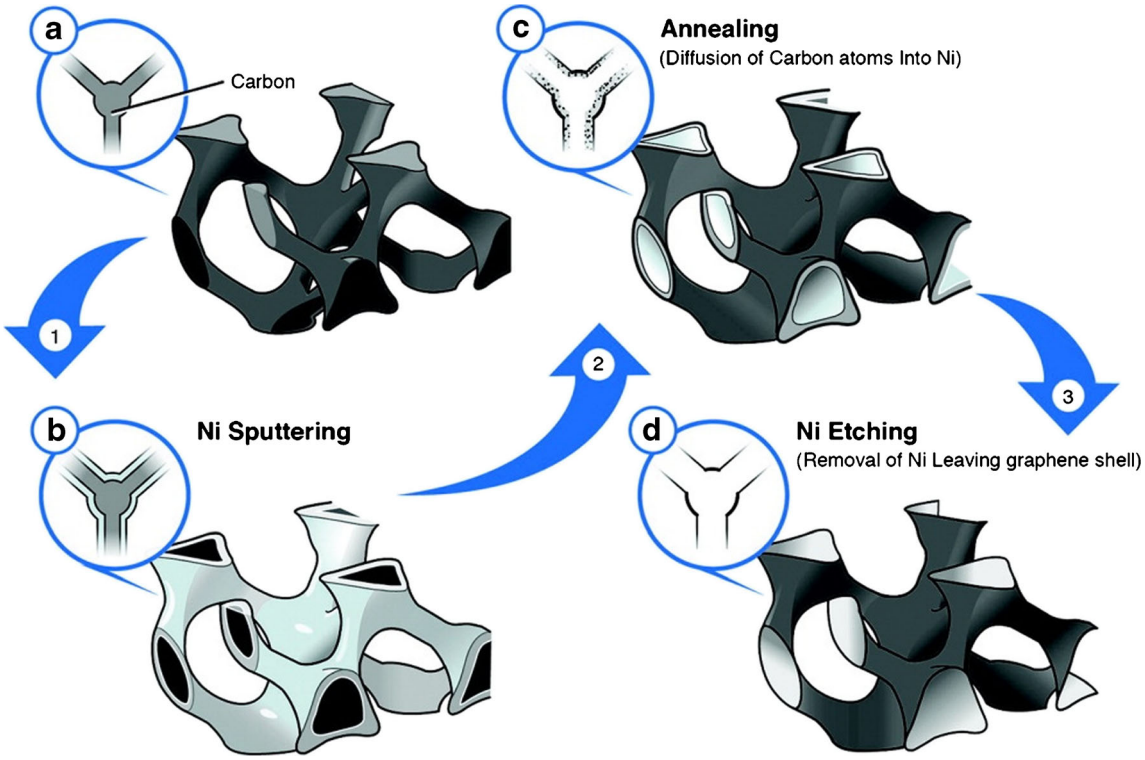

Fig. 3 Schematic drawings illustrating the steps and mechanism for chemical conversion of amorphous porous carbon to 3D graphene: **a** porous carbon, **b** conformal Ni coating, **c** diffusion of carbon into Ni top surface during thermal annealing, and **d** hollow 3D graphene after Ni etching [76]. Copyright (2012) American Chemical Society

was also produced. A rGO-PANI multilayer encapsulated PS sphere was fabricated using a layer by layer assembly method by the interaction of the negative charge rGO and positively charged PANI. The PS core was removed with the help of tetrahydrofuran to get 3D rGO-PANI hollow spheres (Fig. 4) [83]. The fabrication of the 3D graphene by the chemical deposition looks simple and cost-effective. The 3D network is obtained from the GO. GO synthesis and handling are convenient. Due to the hydrophilic nature of GO, it is easily dispersed in the aqueous medium [84]. GO is reduced using

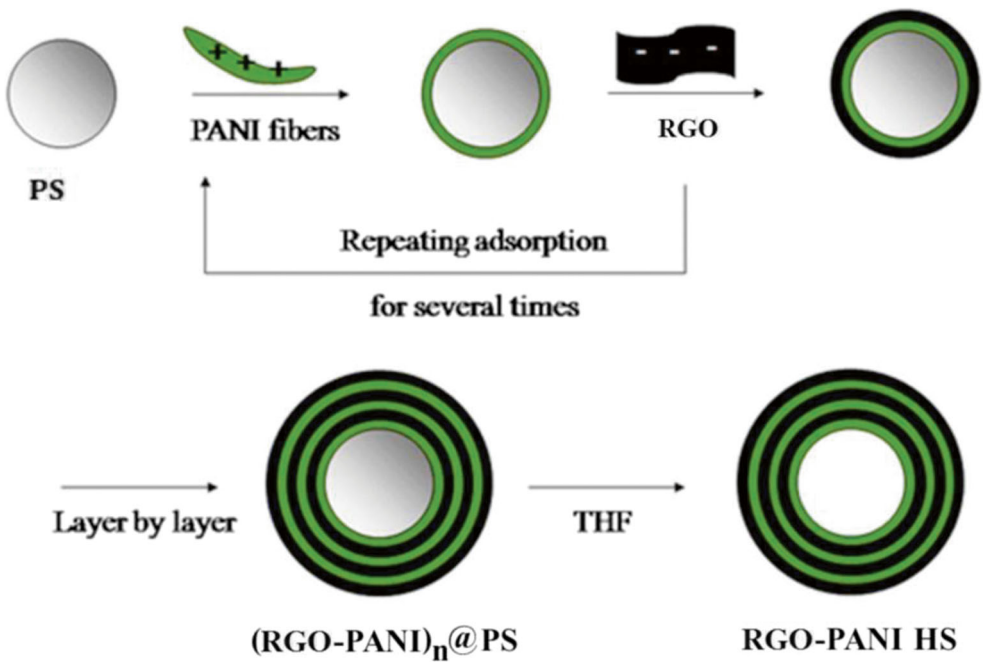

Fig. 4 The illustration of the fabrication procedure of the graphene–PANI hollow spheres (RGO-PANI HS). In the first step, the PANI wrapped PS sphere was formed by mixing negatively charged PS sphered with positively charged PANI. In the second step, the negatively charged RGO sheets self-assembled on PANI@PS by dipping PANI@PS into RGO dispersion. The first and second steps are multiple times repeated to produce (RGO–PANI)n@PS. In the final step, the PS core was removed by dipping in tetrahydrofuran (THF) to generate RGO-PANI HS [83]. Copyright (2015) Elsevier Ltd.

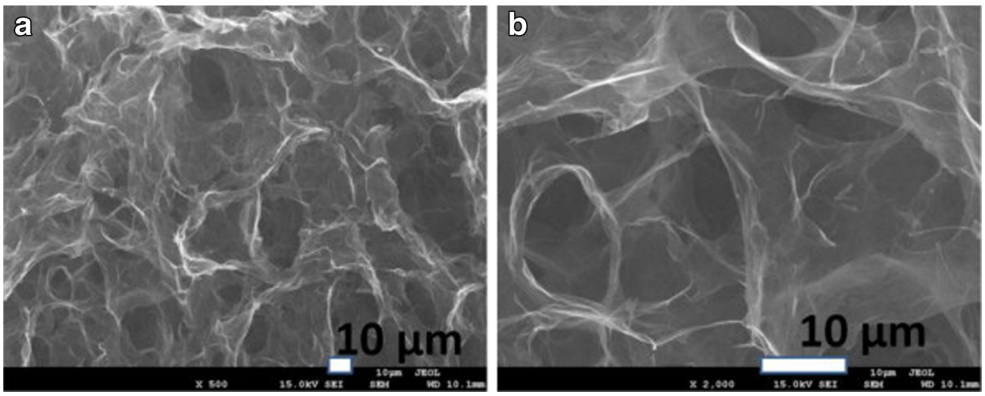

Fig. 5 SEM images the surface of ErGO modified electrode with different magnifications, respectively [88]. Copyright (2013) Elsevier Ltd.

various reducing agents. The reduction of GO can introduce more defects into the rGO. Furthermore, the reduction of the GO not able to restore the pristine graphene network and some oxygen functional group still retained by the surface which substantially affects the performance of the material. Morphology of the 3D rGO is random and poorly controlled by this method.

Direct electrochemical methods

Three-dimensional rGO can be fabricated on the surface of an electrode directly either by applying a constant [85] or by sweeping a range of potential. This method can be utilized to synthesize 3D rGO composites with metals or metallic oxide. The fabrication process for the composites simply consists of two steps. In the first step, the bulk of the GO is directly reduced electrochemically and in second step, the noble metal nanoparticles, metal oxide nanoparticles or conductive polymer are also electrochemically deposited on the surface due to the conductive network of the 3D rGO [86]. 3D rGO and the metallic nanoparticles composite are synthesized by one-step electrochemical reduction. Fan Shi et al. [87] fabricated a three-dimensional rGO–Au nanocomposite on the electrode surface by one step electrochemical co-deposition. The 3D rGO–Au nanocomposite was formed on the surface by sweeping the potential in the range of −1.5 to 0 V using cyclic voltammetry. Similarly, the constant potential (−1.2 V) also has a tendency to provide a 3D interpenetrating porous graphene which is also a one-step process [88]. In another application, the constant potential of −1.3 V was applied to form a 3D rGO film on the CILE surface [89]. The SEM images of the three-dimensionally grown electrochemical rGO can be seen in Fig. 5. The electrochemical methods are the simplest one compared to other methods. 3D rGO films are generated on the surface of the solid electrode simply by applying constant negative or sweeping potential. In this method no special chemical agent is required and the reduction takes place by the exchange of electrons between GO and

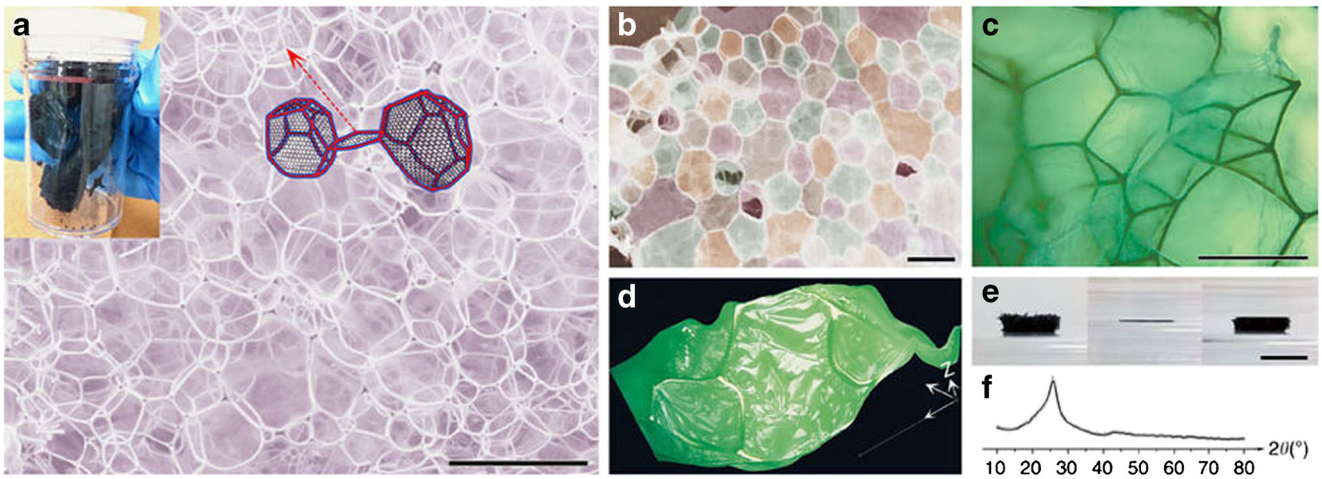

Fig. 6 The 3D bubble-like network of SG. **a** Scanning electron microscope (SEM) image and an optical photo of a 70-mg SG piece obtained at a heating rate of 4 °C min^{-1}. The inset is a reconstructed topology corresponding to the region marked in red for the two connected decahedron–dodecahedron bubbles faced by eight pentagons and two quadrangles, and by eight pentagons, three quadrangles and one heptagon, respectively. **b** SEM image of the flat backside of the SG product with a regular arrangement of connected cells identified by artificial quilt colours. **c**, **d** 2D and 3D optical photos of SG networks. **e** Photos of original compressed and recovered states of a SG specimen. (f) XRD profile of SG. Scale bars, 200 μm (in **a**–**d**) and 1 cm (in **e**) [70]. Copyright (2013) Springer Nature

the electrodes These methods help to avoid the use of dangerous reducing agents and their byproducts [20]. The surface is self-assembled into the 3D network during electrochemical reduction of GO. The major disadvantage of the electrochemical method is the uncontrolled morphology. There is no control on the pore size and the porous network of the 3D rGO.

Other methods

Apart from these methods, several other methods were also implemented for the fabrication of 3D graphene. Xuebin Wang et al. [70] introduced a new method for the bulk production of 3D graphene. 3D self-supported graphene was grown by using a sugar-blowing technique and it was named strutted graphene (SG). It consisted of homogenous and continuous connected networks of the graphitic membrane with μm width graphitic struts spatially supporting the network (Fig. 6). This unique way of synthesis produced 3D graphene with a high mechanical strength, electrical conductivity, elasticity and a huge surface area. This method also provides an opportunity for large-scale production of 3D graphene. The 3D graphene or rGO network can also designed by the 3D printing method [90].

The aforementioned discussion of the synthesis revealed that the 3D graphene architecture can be fabricated in numerous ways and with a variety of materials. The most common approach adopted for the synthesis of a 3D architecture consists of either template or templateless synthesis. Both of these approaches have their own merits and demerits. The template method provides the easiest route to form the 3D network of the graphene. Pore size and the morphology are difficult to control in templateless synthesis while template provides an opportunity to control the porosity of the 3D graphene. The pore size was generated in the range of 600 nm to 4 μm using the PS sphere as a template to obtain 3D porous carbon scaffolds. PS spheres are simply replaced by heat treatment [91]. The 3D metal templates such as Ni-template is used to obtain porous network with the pore size in the range of 50 nm to 1 μm [69]. The most successful method for control of porosity and the morphology of the 3D graphene is a template-directed CVD method. The template with fine pores and range of porosity are required to tune the pore size of the 3D graphene porous network. In CVD methods the template removal during the etching process is a challenge to acquire a defect-free 3D network. Apart from CVD, the templates are used in other synthesis methods including hydrothermal, freeze drying, and support assisted chemical deposition. In these methods, the morphology control is poor compared to the CVD method. Among them, the simplest method is the electrochemically generated 3D network of rGO. In this method, either a constant or sweeping potential is required to produce the rGO. In the electrochemical method, the morphology of the 3D rGO cannot be controlled due to the absence of a template. The freeze drying method is also applied for the templateless synthesis of 3D rGO. GO is the commonly used precursor to attain 3D architecture. GO is reduced by these methods either chemically or electrochemically to improve the electrochemical behaviors. During reduction process, only graphene extraordinary properties partially restored due to retaining of some oxygen functional group. Through these methodologies, it is not an easy job to get a defect-free 3D graphene network. Although, new methods are continuously being introduced, including 3D printing through which 3D free-standing graphene can be achieved with much more control compared with other methods. More serious efforts are required to produce 3D defect-free graphene architectures which are mechanically stable and display the intrinsic characteristics of pristine graphene. Table 2 displays a critical comparison of various methods.

Key features of 3D graphene composites and its application in electrochemical sensing

The 3D hierarchical architectures of graphene include some remarkable physicochemical properties which are very different from both bulk and individual building blocks [55, 94]. Three-dimensional graphene has demonstrated certain advantages which make it an attractive material for the construction of ultrasensitive chemical sensors. Some of the key features of the 3D graphene are described below [31, 67, 78, 88, 95–101].

1) 3D graphene can prevent the agglomeration of planar graphene sheets by overcoming the π–interactions.
2) 3D graphene architecture may also help to restore the intrinsic characteristics of the graphene.
3) 3D graphene can be prepared from free of defects and the intersheet junctions.
4) The 3D interconnected network of the graphene provides the multiple electron paths which facilitate the rapid and sensitive detection of the analyte.
5) The interconnected open porosity of the 3D graphene facilitates the kinetic diffusion and mass transfer of macromolecules.
6) The 3D graphene has low density and high porosity.
7) The 3D monolithic and macroporous graphene foam can act as a free-standing 3D electrode.
8) The small molecules can easily adsorb into 3D graphene hydrogel.
9) The porous network of graphene also facilitates the stable loading of the catalyst and provides a huge surface area for enzyme immobilization.
10) The scaffold of the 3D porous graphene network provides an ideal opportunity to fabricate monolithic composite and hybrid electrodes.

Table 2 Critical comparison of the various methods applied for 3D graphene synthesis

Methods	Precursors	3D develop architecture	Template or templates	Factors	Morphology	Merits	Demerits	Ref.
Hydrothermal	Graphene oxide	Reduced graphene oxide	Template and templateless	Graphene oxide concentration, reaction time,	Controlled (Template), Poor control (Template less)	High electrical conductivity,	Difficult to control morphology and thickness, High temperature, pressure	[62, 92]
CVD	Hydrocarbons, Ethanol	Graphene	Template	Temperature, Template structure, and pore size	Controlled	Fabrication of different morphologies, good mechanical strength, tunability, Freestanding electrode	Expensive, High temperature, template-dependent morphology, Multistep	[62]
Electrochemical deposition	Graphene oxide	Reduced graphene oxide	Templateless	Potential, Concentration of GO, pH	Uncontrolled	Cost-effective, simple and easy handling, Self-assembled	Partially restored graphene intrinsic characteristics, Random morphology	[86]
Freeze drying method	Graphene Oxide	Reduced graphene oxide	Template and Templateless	Freezing rate	Poor control	Without support can be self-assembled into the 3D network, lightweight	Poor control of morphology, multistep, Extreme temperatures are involved	[59, 93]
Support assisted chemical deposition	Graphene	Reduced graphene oxide	Template	Graphene oxide concentration, pH, Heat treatment	Poor control	Large accessible surface area, Electrochemical stability, high specific capacitance, self-assembled	Morphology is not well defined, graphene characteristics partially restored	[81, 82]
Lithography	Carbon	Graphene	Template	Sputtered catalyst,	Controlled	Generates many catalytic active sites, Tunable structural feature, free-standing 3D graphene	Required metal catalyst, Expensive, complex	[76]

Application of 3D graphene and its composite based electrode for electrochemical sensing are further discussed in detail.

Three-dimensional porous graphene-based electrodes

Three-dimensional graphene provides a promising platform for the sensing of various electrochemical analytes. The specific surface area of the 2D electrodes is limited and attempts are being made to construct 3-dimensional electrodes. The 3D graphene network provides multiplexed conductive pathways and offers rapid charge transfer. These factors contribute to enhance the sensitivity of the electrochemical sensor. Highly conductive and monolithic 3D graphene foam was synthesized by CVD and was applied for sensing of dopamine [68]. The sensing of dopamine is challenging due to its close electrooxidation peak with uric acid [102]. The 3D graphene electrodes demonstrate the tendency to distinguish between the dopamine and the uric acid peaks. The sensor displayed a wide linear range of 25 nM to 25 μM. The excellent sensitivity, selectivity and wide linear range of the sensor are attributed to high charge transfer, availability of the high active surface area and π–interactions of the dopamine with graphene. [68]. Similarly, electrochemically synthesized 3D ErGO on AuE displays high conductive channels and strong electrocatalytic behavior for the sensing of dopamine compared to compact 2D ErGO. In compact 2D ErGO provided a limited excess to electrolyte containing dopamine and fewer graphene edges are exposed for the electrocatalysis which is responsible for lower sensitivity [103]. Bo Yu et al. [82] also fabricated a 3D rGO sensor for the sensing of dopamine. A facile way was adopted to attain 3D graphene using a template-assisted self-assembly method in which polystyrene was used as a sacrificial template. The GO and the polystyrene self-assembling were generated by π–interactions. The rGO after removal of the template displayed a 3D network. Electrochemical activity and the sensitivity of the 3D rGO were better when compared to rGO and the poly-(vinylpyrrolidone) (PVP)-stabilized rGO. The enhanced sensitivity of the 3D rGO compared the rGO is due to the open pore structure of the 3D rGO. The sensor displayed sensitivity of 244.17 μA μM^{-1} cm^{-2} at an amperometric potential of +0.3 V which is better [82] than 3D graphene electrodes (0.6196 μA μM^{-1} cm^{-2}). However, the 3D graphene electrode was operated at a lower potential of +0.177 V for the amperometric sensing of dopamine [68]. Chitosan assisted electrochemically reduced 3D GO modified sensors improved the stability and the activity of the immobilized enzyme glucose oxidase (GOD). The fabricated biosensor demonstrated good electrocatalytic activity towards the dissolved oxygen. Direct electrochemistry of immobilized glucose oxidase occurred on the modified electrode which leads to the conversion of GOD(FAD) to GOD($FADH_2$) due to fast electron transfer between the graphene-modified electrode and the enzyme. It electrocatalyzed the dissolved oxygen reduction which leads to the regeneration of GOD(FAD) from GOD($FADH_2$). In this way, the electrocatalytic reaction can be repeated again and again. The reduction current of the air saturated solution decreased with glucose spiking due to the interaction of glucose with GOD(FAD). This helps to attain a wide linear range of the glucose. The fabricated biosensor was highly selective for glucose in the presence of potentially interfering species [88]. In another work, the 3D rGO was generated on the surface of the CILE using the direct electrochemical method to immobilize the hemoglobin for biosensor fabrication. Hemoglobin displayed a direct electrochemistry on the surface of the 3D rGO/CILE. The biosensor catalyzed the reduction of trichloroacetic acid in the absence of electron mediators [89]. In another work, the graphene aerogel@octadecylamine-functionalized carbon quantum dots modified GCE displayed a wide linear response of 0.001–10 μM for acetaminophen determination [104]. The 3D hollow graphene balls were also used for the sensing of levodopa in the presence of uric acid [105].

The fast charge transfer of the 3D graphene composite also assists the sensor for the real-time application. For example, the real-time application of the nitric oxide is challenging due to trace level of the endogenous NO and its reaction with oxygen is critically fast with very short half-life. A sensor with fast response time is only suitable for real-time sensing [106]. The 3D rGO/IL nanocomposite was prepared by mixing 3D rGO and the 1-butyl-3-methylimidazolium hexafluorophosphate ionic liquid to fabricate a carbon paste electrode for sensitive sensing of NO. During amperometric measurements, the steady state current was achieved after spiking of the NO in less than 4 s which made it a good candidate for the in-situ or in-vivo applications [107]. Table 3 demonstrated the figure of merits of 3D porous graphene-based electrodes.

3D graphene metals and metals oxide composite modified electrodes

The composites of 3D graphene with metals nanoparticles offer a platform for the sensitive and selective sensing of various targeted species. The metal nanoparticles act as a catalyst during electrochemical reactions [108, 109]. The metallic nanoparticle modified sensor performance is affected due to the agglomeration and dissolution of the electrocatalyst during the catalytic reaction. In this regard, either graphene or other carbon materials are used as a support [110] to improve the catalyst durability, electroactive surface area, and surface sensitivity. The cooperative interaction of graphene and metal nanoparticles promotes the electron transfer. However, the catalyst performance, electrolyte diffusion, and the electroactive surface area are compromised due to the agglomeration of graphene by π–interactions [111]. 3D graphene architecture is the best alternative to fix the issue of 2D graphene

Table 3 Figure of merits of three-dimensional porous graphene-based electrodes. PB stands for phosphate buffer.

Modified electrode	Analyte	Technique	Sensing medium	pH	Working potential vs. Ag/AgCl (V)	Sensitivity ($\mu A \cdot \mu M^{-1} \cdot cm^{-2}$)	Linear range (μM)	LOD (μM)	Application	Ref.
3D graphene electrode	Dopamine	Amperometry	0.1 M PB	7.2	+0.177	0.6196	0.025-25	–	–	[68]
3D-rGO/GCE	Dopamine	Amperometry	0.1 M PB	7.0	+0.3	244.17	5–1000	0.17	–	[82]
3D ErGO/AuE	Dopamine	Amperometry	0.1 M PB	7.0	–	–	0.1–10	0.1	Human serum	[103]
3-D rGO/IL nano-composite	Nitric Oxide	Amperometry	0.1 M PB	7.0	–	11.2	Up to 16	0.016	–	[107]
CS-GOD-ErGO/GCE	Glucose	Amperometry	0.01 M PB	7.3	−0.45	6.82×10^{-3}	20–3200	1.7	–	[88]
CTS/Hb/3D-rGO/CILE	Trichloroacetic acid	CV	0.1 M PB	3.0	–	–	400–26,000	130	water and drug samples	[89]

agglomeration. A immunosensor was fabricated for the detection of carcinoembryonic antigens (CEA) by using 3D-AuNP/rGO. The immunosnesor was achieved by immobilizing the primary antibodies (Ab1) into a 3D porous network of rGO. The CEA was attached to the sensor by an antigen-antibody relation. The electrochemical signal was generated with the assist of thionine and horseradish peroxidase (Fig. 7). The immunosensor demonstrated a very low limit of detection of 0.35 pg mL^{-1} for CEA [79]. The combination of 3D graphene hydrogel and Au NPs was also applied to the simultaneous detection of AA, DA, and UA [112]. The bimetallic nanoparticles of PdCu were encapsulated and dispersed within the 3D

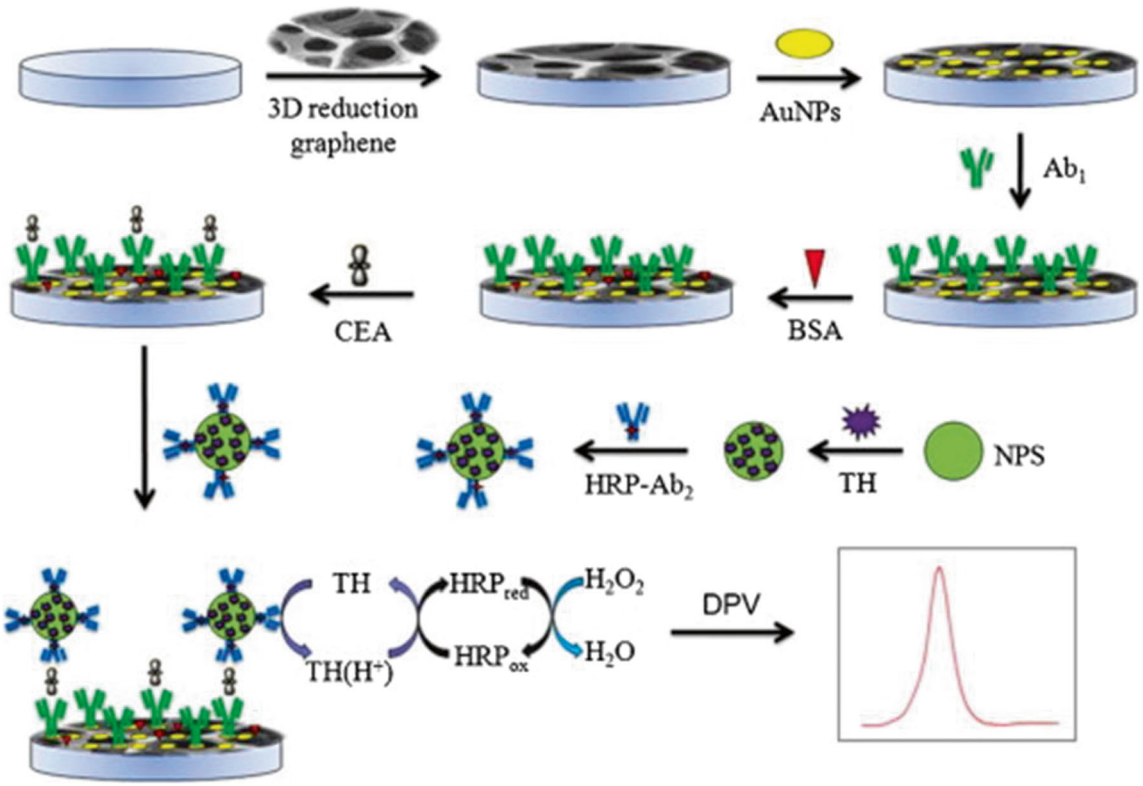

Fig. 7 Fabrication process of HRP-Ab2/TH/NPS nanomaterials and measurement protocol of the electrochemical immunosensor. In the first step, 3D-AuNPs/GN deposited on the GCE then incubated for 35 min and washed to remove unspecific adsorption. After that, it was incubated in 1.0 wt% BSA for 30 min at room temperature. In next step, Ab1/3D-AuNPs/GN/GCE immunosensor, was incubated with CEA standard antigen and unbounded CEA molecule remove by extensive washing. A sandwich immunocomplex was constructed by dropping HRP-Ab2/TH/NPS onto the modified electrode. DPV was used for sensing of CEA [79]. Copyright (2013) Elsevier B.V.

interconnected network of rGO. The 3D rGO provided an opportunity for the uniform dispersion of the PdCu NPs on both sides of the rGO sheets. The synergistic effect of 3D rGO and the bimetallic nanoparticles significantly improved the electrocatalytic oxidation of glucose and its selectivity over potential interfering species [71]. Similarly, the 3D porous graphene foam was used for the incorporation of bimetallic nanoparticles of platinum and ruthenium which act as a nanocatalyst for hydrogen peroxide determination. The ultra-hollow structure of graphene foam with its large number of active sites provides the opportunity for the uniform dispersion of bimetallic nanoparticles. Sometimes amperometric biosensors are inaccurate for finding out the concentration of H_2O_2 due to their low sensitivity. The porous 3D graphene provides rapid mass transport of the reactant to the nanocatalyst and enhances the sensitivity for H_2O_2. The sensitivity of the bimetallic nanoparticle sensor with 2D graphene was 0.7954 which were substantially improved to 1.0231 $\mu A \cdot \mu M^{-1} \cdot cm^{-2}$ by replacing graphene with 3D graphene foam. The detection limit was also improved significantly from 0.355 to 0.04 μM [113]. The 3D graphene as a free-standing electrode demonstrated a high catalytic activity for methanol oxidation compared to the 3D scaffold of carbon fiber [114].

The combination of metallic oxide and 3D graphene was also applied to certain analytes in which metallic oxide acts as a catalyst while 3D graphene assists the rapid charge transfer during the electrochemical reaction. The cobalt oxide (Co_3O_4) nanowires on the 3D graphene were used for the fabrication of a monolithic free-standing electrode which is applied to the enzymeless sensing of glucose. The Co_3O_4 is proficient enough to catalyze the glucose oxidation and enable the electrode to sense glucose without other mediators or enzymes. The 3D graphene/Co_3O_4 composite due to the superior mechanical strength of the graphene, it can be used as a free-standing electrode with better sensitivity for glucose sensing [31]. In another work, in situ ZnO nanorods were fabricated on CVD grown 3D graphene. The high conductivity of the 3D graphene and the electroactive properties of the ZnO facilitate the rapid charge transfer which is required for dopamine sensing [60]. The figure of merits for the 3D graphene metals and metals oxide composite modified electrodes are described in Table 4.

3D graphene and organic polymer composite modified electrodes

The combination of polymers with graphene is generally used to improve the selectivity and the sensitivity of the sensor [115, 116]. Mostly, conductive polymers are used for the fabrication of electrochemical sensors [117]. Conductive polymers are a class of polymers which contain numerous sp^2 hybridized carbon atoms and their large resonating structure allows the delocalized transport of charge carriers [118]. The hybrid of 3D graphene with polymer composite was also used for the sensing of various analytes with improved selectivity. For example, the oligonucleotides display a great tendency for specific interaction with metal ions. The DNA makes a stable and strong complex with mercury ions through thymine [119]. The thymine–Hg^{2+}–thymine complexes were used for the sensing of mercury ions [120]. A 3D-rGO@PANI nanocomposite was used to fabricate a biosensor for the selective determination of mercury ions by immobilizing the DNA. The 3D rGO substantially enhanced the electrochemical performance and the specific surface area of the nanocomposite for the immobilization of DNA. The biosensor was selective towards the mercury ions as it binds with T-rich DNA by making T-Hg^{2+}-T coordination which increased the biosensor impedance. The biosensor was very sensitive for Hg^{2+} with a limit of detection 0.035 nM [59]. Similarly, a biosensor was obtained by immobilizing the DNA on the nanocomposite of 3D rGO and plasma-polymerized propargylamine (3D-rGO@PpPG) for the sensitive and selective determination of Hg^{2+} [120].

Fei Liu et al. [78] introduced a 3D rGO micropillar electrochemical biosensor consist of tyrosinase enzyme for the sensitive detection of phenol. In the microfluidic channels, 3D PDMS micropillars were patterned and the surface was modified with 3-aminopropyltriethoxysilane. GO adsorbed on the PDMS through electrostatic force of attraction and reduced with hydrazine to attain a 3D rGO conductive architecture (Fig. 8). Tyrosinase enzymes catalyzed the introduced phenol into catechol and catechol was further oxidized into o-quinone which electrochemically reduced back to catechol. The tyrosinase enzyme-mediated biosensor was specific for phenol which reduces the chance of interference.

In some cases, the polymer was introduced onto the surface of 3D graphene to act as a linker for further attachment of functional groups. Hydrophilicity is one of the factors for the loading and preservation of the bioactivity of the biomolecules during bioanalysis. The 3D graphene foam is highly hydrophobic. The polymer such as polydopamine (pDA) performs two functions; first, it imparts the hydrophilic character to 3D graphene and, second, act as a linker for the attachment of other groups. The dopamine can polymerize in-situ in the alkaline medium on the 3D graphene to act as a linker and render the hydrophilic character to the surface [121]. The polydopamine efficiently adhere to the surface of the graphene via π–stacking interaction [64]. It is established that ambiphilic pDA have strong bond formation tendency with various hydrophilic and hydrophobic surfaces using their ortho-dihydroxy-phenyl functional groups [121]. The adhered pDA provides ample reactive handles that have the capabilities to conjugate with thiol- or amine-containing molecules via Michael addition or Schiff base reactions [64]. Jiyang Liu

Table 4 Figure of merits of 3D graphene metals and metals oxide composite modified electrodes. PB stands for phosphate buffer

Modified electrode	Analyte	Technique	Sensing medium	pH	Working potential, Vs. Ag/AgCl (V)	Sensitivity ($\mu A \cdot \mu M^{-1} \cdot cm^{-2}$)	Linear range (μM)	LOD (μM)	Application	Ref.
PdCu/rGO modified ITO	Glucose	Amperometry	0.1 M NaOH + 0.15 M KCl	–	−0.4	0.048	1– 18,000	20	Human serum sample	[71]
3D graphene/Co_3O_4 composites	Glucose	Amperometry	–		0.58	3.39	Up to 80	<0.025	–	[31]
graphene/ZnO hybrid electrode	Dopamine	Amperometry	0.1 M PB	7.2	–	0.01518	Up to 2.0	~ 0.01	–	[60]
graphene/ZnO hybrid electrode	$K_3[Fe(CN)_6]$	Amperometry	0.1 M PB	7.2	0.1	7×10^{-5}	Up to 800	~ 1	–	[60]
PtRu/3D GF	H_2O_2	Amperometry	0.1 M PB saline containing 0.15 M KCl	7.4	0.365	1.0231	0–20	0.04	–	[113]

et al. [121] used the polydopamine linker to functionalize the concanavalin A monolayer on the 3D graphene. The horseradish peroxidase (HRP)-labeled antibody (anti-CEA) was immobilized further to develop a 3D immunosensor which have the capability to sense carcinoembryonic antigen with wide linear range and very low limit of detection (Fig. 9) [121]. In another example, polydopamine linker on the 3D graphene surface act as a linker for the functionalization of the thionine molecules which has the capability to efficiently mediate the enzymeless reduction of H_2O_2. Thionine is oxidized to facilitate the reduction of H_2O_2 to H_2O and reduced back to thionine via electron transfer on the electrode surface. It was applied for real-time sensing of H_2O_2 released from cancer cells in response to a pro-inflammatory stimulant [64]. Table 5 demonstrates the figure of merits of 3D graphene and organic polymer composite modified electrodes.

CNT-decorated 3D graphene-based electrodes

The synergistic effect of CNT and graphene helps to attain the robust and the flexible electrodes [116]. The SWCNTs can act as the spacer, binder and conductive additive to the composites [122]. The CNTs decoration of 3D graphene further improves the electroactivity of the surface. A ferrocene-branched chitosan (Fc-CS), single-walled carbon nanotubes (SWCNTs) and glucose oxidase (GOD) modified Fc-CS/SWCNTs/GOD/3DG electrode was used for the electrochemical sensing of glucose. The immobilization of the ferrocene grafted chitosan on the 3D graphene was stable and retained its original activity. The SWCNTs in Fc-CS matrix act as nanowires to improve the conductivity and electron transfer of the biocomposite film. The biosensor was fabricated by immobilizing the biocomposite which contained a glucose oxidase (GOD) using a one-step electrodeposition on the 3D graphene foam [123]. The chitosan solubility is pH dependent and at a higher pH (> 6.3) it becomes insoluble [124, 125]. A 3D graphene electrode was dipped into a solution containing the GOD, SWCNTs, and Fc-CS. At an applied potential of −1.5 V, the pH was increased near the electrode surface due to the reduction of H^+ to H_2. The chitosan became insoluble as the local pH exceeded 6.3. As a result, the GOD enzyme and SWCNTs incorporated into the CS Fc-CS hydrogel were electrodeposited onto the 3D graphene electrode. This provides the easiest way to fabricate a reagentless enzymatic glucose sensor by bio-modification of monolithic 3D-G foam using a one-step CS electrodeposition technique [123]. As discussed, the 3D graphene porous network can also use as a template for the loading of the various nanomaterial to fabricate the graphene-based composite electrodes for enhancing the sensing capability of the sensor. Xiehong Cao et al. [67] also synthesized 3D graphene architecture in which various nanomaterial successfully deposited. The combination of the entangled MWCNTs and the 3D graphene porous network displayed a hierarchical structure. At the edges, numerous protruded MWCNT tips were observed. These extended tips serve as electron transfer conduction channels and enhance the activity towards the electrochemical reaction. The functionalization of Pt NPs on the 3DGN/MWCNTs significantly improved the electrochemical activity of the composite towards H_2O_2. Overall these composites reduce the overpotential compared to 3D graphene. Table 6 describes the figure of merits of functionalized 3D graphene and MWCNTs-decorated 3D graphene-based electrodes.

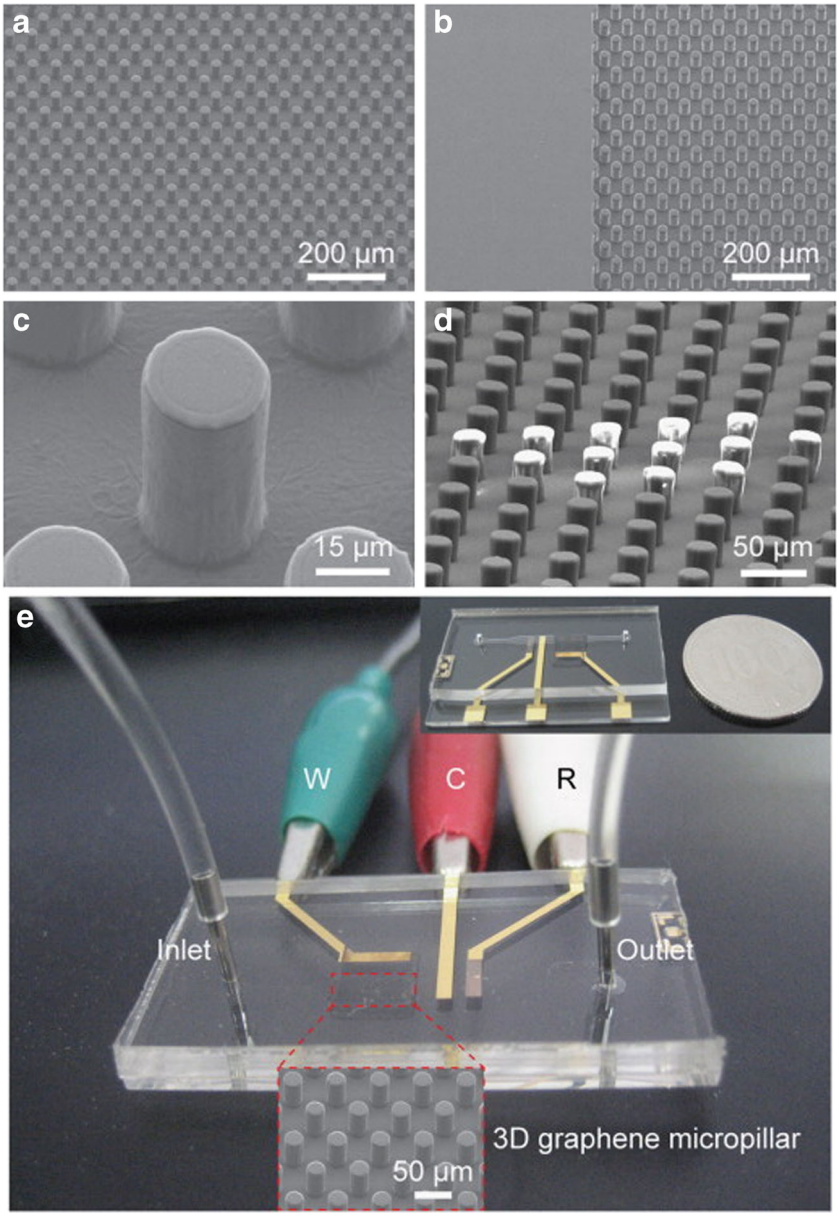

Fig. 8 **a**, **b** Low- and **c** high-magnification SEM images of the 3D graphene micropillars. **d** The PDMS micropillars uncovered with graphene are shown bright due to the charging effect. **e** Digital image of the graphene micropillar integrated electrochemical sensor device for phenol detection [78]. Copyright (2013) Elsevier B.V.

Miscellaneous

Apart from the above combination, the 3D graphene can also combine with other materials to enhance the electroactivity of the sensors. The 3D graphene or rGO is doped with heteroatoms to improve the electrochemical behavior of the graphene [126, 127]. Generally, those heteroatoms are used for doping in graphene which has a close resemblance in electronegativity and atomic structure, to carbon [128]. The 3D phosphorous doped rGO was synthesized by a hydrothermal and annealing treatment. The 3D porous network of the rGO and the phosphorous doping synergistic effect enable the sensor to sense trace level H_2O_2 released from the living cells (HeLa) [127]. Similarly, the 3D ammonia doped porous rGO/CuO modified sensor was applied to the non-enzymatic sensing of glucose. The composite was achieved on the gold electrode surface by directly applying the DC voltage in an ammonia doped porous rGO and $Cu(ClO_4)_2$ suspension using electrophoretic deposition. The film thickness was controlled by the deposition time [126]. In another work, 3D nitrogen-doped graphene was fabricated which provided a favorable environment for the immobilization of the single-stranded DNA probe [129]. In some cases, the graphene was used with other biomolecules or nanomaterial to construct 3D nanocomposites. The ZnO nanorods were used for the fabrication of a 3D rGO/Ni hybrid electrode for a non-enzymatic glucose sensor [130]. In another work, the 3D composite was fabricated on the surface of the gold electrode using graphene and DNA.

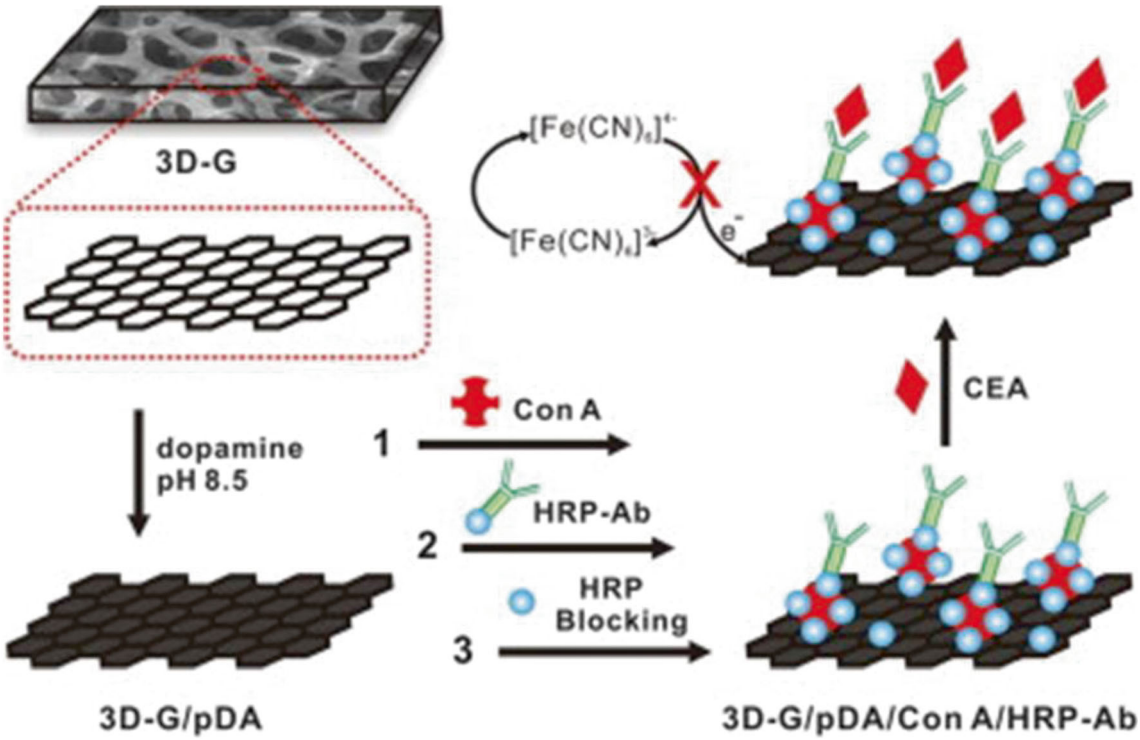

Fig. 9 Schematic illustration of the fabrication and CEA detection process of the immunosensor. 3D-G/pDA formed by the in-situ polymerization of dopamine in alkaline medium. The concanavalin A (Con A) was covalently immobilized by linking through polydopamine on the electrode surface. After that, the horseradish peroxidase (HRP)-labeled antibody (anti-CEA) was efficiently immobilized to demonstrate the recognition interface [121]. Copyright (2014) Elsevier B.V.

The 3D structure was built using a layer by layer assembly to construct a sensitive and selective sensor for dopamine sensing [94]. Figure of merits of the miscellaneous 3D graphene-based electrodes are described in Table 7.

Future perspectives, challenges, and conclusion

After the day of isolation, a significant progress in graphene material is made and with the passage of time, the new approaches are being introduced to effectively use graphene in different applications. Apart from the huge progress in graphene, still it is difficult to prepare graphene in bulk which is fully displaying its intrinsic properties. The key challenges are the agglomeration of graphene sheets and the defects that are generated during the synthesis. 3D graphene architecture is the newly introduced morphology of the planar graphene which is continuously getting attention from a couple of years in the different field. It has full potential to prove a promising electrode material for the fabrication of sensitive and selective electrochemical sensors for trace level quantification of the various analytes. 3D graphene not only possesses the properties of the intrinsic graphene but also provides some additional

Table 5 Figure of merits of 3D graphene and organic polymer composite modified electrodes. PB: phosphate buffer

Modified electrode	Analyte	Technique	Sensing medium	pH	Working potential, Ref. Ag/AgCl (V)	Sensitivity ($\mu A \cdot \mu M^{-1} \cdot cm^{-2}$)	Linear range (μM)	LOD (μM)	Application	Ref.
3D-rGO@PANI/gold electrode	Hg^{2+}	Electrochemical impedance spectroscopy	0.1 M PB	7.4	0.22	–	0.0001–0.1	0.000035	River water	[59]
3D-rGO@PpPG	Hg^{2+}	DPV	PB	7.4	–	–	0.0001–0.2	0.00002	Water samples	[120]
3D rGO micropillar integrated electrochemical sensor	Phenol	Amperometry	0.1 M PB	–	−0.1	3.9×10^{-3}	0.05–2	0.05	–	[78]

Table 6 Figure of merits of functionalized 3D graphene and MWCNTs-decorated 3D graphene-based electrodes

Modified electrode	Analyte	Technique	Sensing medium	pH	Working potential, Ref. Ag/AgCl (V)	Sensitivity ($\mu A \cdot \mu M^{-1} \cdot cm^{-2}$)	Linear range (μM)	LOD (μM)	Application	Ref.
Fc-CS/SWNTs/GOD/3DG electrode	Glucose	Amperometry	0.1 M PB	7.0	0.4	–	5–19,800	1.2	–	[123]
3D graphene /PtNP composite electrode	H_2O_2	Amperometry	0.01 M PB	7.4	0.45	–	0.167–7.486	0.125	–	[67]
3D graphene /MWCNT composite electrode	H_2O_2	Amperometry	0.01 M PB	7.4	0.45	–	20–280	6.54	–	[67]
3D graphene /MWCNT/PtNP composite electrode	H_2O_2	Amperometry	0.01 M PB	7.4	0.45	–	0.025–6.3	0.0086	–	[67]
3D graphene /MnO_2 composite electrode	H_2O_2	Amperometry	0.01 M PB	7.4	0.45	–	0.38–13.46	0.27	–	[67]
3D graphene/pDA/TH electrode	H_2O_2	Amperometry	0.05 M PB	6.0	−0.25	0.1697	0.4–660	0.08	live cancer cells	[64]

benefits. It prevents the agglomeration of the graphene sheets and allows the free movement of the electrolyte into the porous graphene network. The analyte has more contact with the 3D graphene compared to 2D planar graphene. It also offers facile and more stable loading of catalyst and enzyme due to porous network, for the fabrication of electrochemical sensor as well as a biosensor. Although in numerous sensing applications, the 3D graphene was fabricated on the surface of the conventional electrode, nevertheless, the free-standing 3D graphene has an obvious advantage over 2D planar graphene network, as it can directly use as an electrode.

The 3D graphene porous network and the huge surface area enable the stable composites with other active materials to achieve the desired results. The various composites of 3D graphene are introduced with other nanomaterials including metallic/metallic oxide nanoparticles, conductive polymers, and MWCNTs. The 3D graphene provides better dispersion of the nanoparticles and helps to improve their electrocatalytic behavior. The 3D graphene also provides an opportunity to functionalize the surface of the graphene with different biomolecules to enhance the sensitivity and the selectivity of the sensors towards specifically targeted analytes.

Actually, all the unique properties of the 3D graphene depend on the efficient preparation of the material. The 3D G/rGO was obtained by several methods, including electrochemical methods [86], template-assisted methods [66, 131] and a self-assembled strategy [132, 133]. Mostly graphene is referred to rGO and the precursor is the GO. The GO is widely used due to its more feasible synthesis route and it can easily disperse into the aqueous medium. It can be reduced very easily by chemical or electrochemical methods [134, 135]. The rGO electrochemical properties are significantly different from graphene due to the partial removal of the oxygen-containing functional groups. The sp^2 planar structure of the graphene cannot fully restore due to the retaining of the oxygen-containing functional groups. Synthesis of graphene from GO by the synthetic route is extremely difficult [136]. Another challenge to obtain a 3D graphene network with controlled porosity. In templateless methods, the porosity is difficult to control and 3D graphene network grown with random morphology. The pore size of 3D porous network somehow controlled using the template which provides an opportunity to fabricate the porous material according to the guest molecule size. 3D porous carbon scaffolds with few nanometers to several micrometers pore size were fabricated using PS spheres as a template for bacterial cells confinement [91]. A graphene skeleton with a large pore size of 100–200 μm is also reported [137] A commonly used method for obtaining

Table 7 Figure of merits of miscellaneous 3D graphene-based electrodes

Modified electrode	Analyte	Technique	Sensing medium	pH	Working potential, Ref. Ag/AgCl (V)	Sensitivity ($\mu A \cdot \mu M^{-1} \cdot cm^{-2}$)	Linear range (μM)	LOD (μM)	Application	Ref.
Au/ammonia-doped-prGO/CuO electrode	Glucose	Amperometry	0.1 M NaOH	–	0.50	1.21	0.25–6000	0.25	Human serum samples	[126]
3D-PrGO/GCE	H_2O_2	Amperometry	0.1 M PB	7.4	−0.4	–	0.2–41,200	0.17	living HeLa cells	[127]

3D graphene with controlled morphology is the template-assisted CVD method [138]. The template in the CVD allowed better tuning of the porosity and the morphology of the 3D graphene. 3D nanoporous graphene with pore size of 50 nm to 1 μm synthesized using Ni-based nanotemplates [69]. However, the removal of the template without damaging the 3D graphene network is a challenge and most defects are generated during its removal which affects the sensor performance. The 3D graphene can also obtain by a sugar blowing technique with random geometry and the pore size [139]. It is obvious that the performance of the 3D graphene-based sensors depends on the efficient synthesis of the defect-free graphene network. The high level of geometry and shape control of the 3D graphene was attempted by 3D printing strategies [140]. Apart from all these methods, more exploration is required to introduce new facile methods for the synthesis of 3D free-standing graphene networks without any defects. 3D graphene, along with other widespread applications, has also been explored in electrochemical sensing. However, it is in its infancy stage regarding the fabrication of electrochemical sensors and very few applications have been reported including the sensing of biomolecules, organic and inorganic pollutants. 3D graphene material has great potential in the field of sensing for fabrication of highly selective and sensitive electrochemical sensors. Due to its unique porosity and 3D network, it provides the improved potential for loading the desired biomolecules for biosensor fabrication. The large biomolecules can also easily access to the tuned pore size of the 3D graphene porous network. This material can bring more useful results by the functionalization of the 3D graphene surface for specific analytes. The functionalization assists the 3D graphene to preconcentrate the targeted analyte into the porous network. This result into a substantial improvement in sensor selectivity, as well as sensitivity, compared to its 2D planar counterpart.

There is no doubt that 3D graphene is an extraordinary electrode material but some serious challenges are associated with the fabrication of 3D graphene porous network. The unique and extraordinary characteristics of the 3D graphene are only depends upon the successful construction of the material. The porosity of the material until now is not precisely controlled and pore size is distributed in the range of nm to μm. Moreover, during preparation, many defects are generated in the architecture which severely affects their performance in the electrochemical sensing. The mechanical stability of the 3D network of the graphene still needs to be fixed to make them valuable sensing tool. There is also need to put more focus on the determination of defects during construction the material and find outs the methods to eliminate them. This will help to improve the mechanical stability and electrochemical behavior of the 3D graphene electrodes. More theoretical and experimental exploration of 3D graphene with other nanocomposite is required to obtain the optimum synergistic effect for selective and sensitive sensing of the analytes. 3D graphene has a promising future in the field of electrochemical sensing for the fabrication of low cost and sensitive sensors.

Acknowledgements The authors gratefully acknowledge the support provided by the Chemistry Department at King Fahd University of Petroleum and Minerals (KFUPM).

Compliance with ethical standards The author(s) declare that they have no competing interests.

References

1. Geim AK, Novoselov KS (2007) The rise of graphene. Nat Mater 6:183–191. https://doi.org/10.1038/nmat1849
2. Yang S, Li Y, Wang S et al (2018) Advances in the use of carbonaceous materials for the electrochemical determination of persistent organic pollutants. A review. Microchim Acta 185:112. https://doi.org/10.1007/s00604-017-2638-9
3. Goutham S, Bykkam S, Sadasivuni KK et al (2018) Room temperature LPG resistive sensor based on the use of a few-layer graphene/SnO2 nanocomposite. Microchim Acta 185:69. https://doi.org/10.1007/s00604-017-2537-0
4. Kawde A-N, Baig N, Sajid M (2016) Graphite pencil electrodes as electrochemical sensors for environmental analysis: a review of features, developments, and applications. RSC Adv 6:91325–91340. https://doi.org/10.1039/C6RA17466C
5. Geim AK (2009) Graphene: status and prospects. Science (80-) 324:1530–1534. https://doi.org/10.1126/science.1158877
6. Bollella P, Fusco G, Tortolini C et al (2017) Beyond graphene: electrochemical sensors and biosensors for biomarkers detection. Biosens Bioelectron 89:152–166. https://doi.org/10.1016/j.bios.2016.03.068
7. Nair RR, Blake P, Grigorenko AN et al (2008) Fine structure constant defines visual transparency of graphene. Science (80-) 320:1308–1308. https://doi.org/10.1126/science.1156965
8. Cao X, Yin Z, Zhang H (2014) Three-dimensional graphene materials: preparation, structures and application in supercapacitors. Energy Environ Sci 7:1850–1865. https://doi.org/10.1039/C4EE00050A
9. Pumera M, Ambrosi A, Bonanni A et al (2010) Graphene for electrochemical sensing and biosensing. TrAC Trends Anal Chem 29:954–965. https://doi.org/10.1016/j.trac.2010.05.011
10. Brownson DAC, Banks CE (2010) Graphene electrochemistry: an overview of potential applications. Analyst 135:2768. https://doi.org/10.1039/c0an00590h
11. Gan T, Hu S (2011) Electrochemical sensors based on graphene materials. Microchim Acta 175:1–19. https://doi.org/10.1007/s00604-011-0639-7
12. Martín A, Escarpa A (2017) Tailor designed exclusive carbon nanomaterial electrodes for off-chip and on-chip electrochemical detection. Microchim Acta 184:307–313. https://doi.org/10.1007/s00604-016-2020-3
13. Stankovich S, Dikin DA, Dommett GHB et al (2006) Graphene-based composite materials. Nature 442:282–286. https://doi.org/10.1038/nature04969
14. Cinti S, Arduini F (2017) Graphene-based screen-printed electrochemical (bio)sensors and their applications: efforts and criticisms. Biosens Bioelectron 89:107–122. https://doi.org/10.1016/j.bios.2016.07.005

15. Zhu C, Yang G, Li H et al (2015) Electrochemical sensors and biosensors based on nanomaterials and nanostructures. Anal Chem 87:230–249. https://doi.org/10.1021/ac5039863
16. Mkhoyan KA, Contryman AW, Silcox J et al (2009) Atomic and electronic structure of graphene-oxide. Nano Lett 9:1058–1063. https://doi.org/10.1021/nl8034256
17. Chen D, Feng H, Li J (2012) Graphene oxide: preparation, functionalization, and electrochemical applications. Chem Rev 112:6027–6053. https://doi.org/10.1021/cr300115g
18. Baig N, Kawde A-N (2015) A novel, fast and cost effective graphene-modified graphite pencil electrode for trace quantification of <scp>l</scp> −tyrosine. Anal Methods 7:9535–9541. https://doi.org/10.1039/C5AY01753J
19. Gómez-Navarro C, Meyer JC, Sundaram RS et al (2010) Atomic structure of reduced graphene oxide. Nano Lett 10:1144–1148. https://doi.org/10.1021/nl9031617
20. Pei S, Cheng H-M (2012) The reduction of graphene oxide. Carbon N Y 50:3210–3228. https://doi.org/10.1016/j.carbon.2011.11.010
21. Sun H, Wu L, Wei W, Qu X (2013) Recent advances in graphene quantum dots for sensing. Mater Today 16:433–442. https://doi.org/10.1016/j.mattod.2013.10.020
22. Wu C, Huang X, Wang G et al (2013) Highly conductive nanocomposites with three-dimensional, compactly interconnected graphene networks via a self-assembly process. Adv Funct Mater 23:506–513. https://doi.org/10.1002/adfm.201201231
23. Dreyer DR, Park S, Bielawski CW, Ruoff RS (2010) The chemistry of graphene oxide. Chem Soc Rev 39:228–240. https://doi.org/10.1039/B917103G
24. Joung D, Khondaker SI (2013) Structural evolution of reduced graphene oxide of varying carbon sp 2 fractions investigated via coulomb blockade transport. J Phys Chem C 117:26776–26782. https://doi.org/10.1021/jp408387b
25. Wang Y, Hu A (2014) Carbon quantum dots: synthesis, properties and applications. J Mater Chem C 2:6921. https://doi.org/10.1039/C4TC00988F
26. Pan D, Zhang J, Li Z, Wu M (2010) Hydrothermal route for cutting graphene sheets into blue-luminescent graphene quantum dots. Adv Mater 22:734–738. https://doi.org/10.1002/adma.200902825
27. Zhang C, Wei K, Zhang W et al (2017) Graphene oxide quantum dots incorporated into a thin film nanocomposite membrane with high flux and antifouling properties for low-pressure nanofiltration. ACS Appl Mater Interfaces 9:11082–11094. https://doi.org/10.1021/acsami.6b12826
28. Sinha A, Dhanjai JR et al (2018) Voltammetric sensing based on the use of advanced carbonaceous nanomaterials: a review. Microchim Acta 185:89. https://doi.org/10.1007/s00604-017-2626-0
29. De Adhikari A, Oraon R, Tiwari SK et al (2018) CdS-CoFe 2 O 4 @Reduced graphene oxide nanohybrid: an excellent electrode material for supercapacitor applications. Ind Eng Chem Res 57:1350–1360. https://doi.org/10.1021/acs.iecr.7b04885
30. He Y, Chen W, Li X et al (2013) Freestanding three-dimensional graphene/MnO 2 composite networks as ultralight and flexible supercapacitor electrodes. ACS Nano 7:174–182. https://doi.org/10.1021/nn304833s
31. Dong X-C, Xu H, Wang X-W et al (2012) 3D graphene–cobalt oxide electrode for high-performance supercapacitor and enzymeless glucose detection. ACS Nano 6:3206–3213. https://doi.org/10.1021/nn300097q
32. Zhang H, Gai P, Cheng R et al (2013) Self-assembly synthesis of a hierarchical structure using hollow nitrogen-doped carbon spheres as spacers to separate the reduced graphene oxide for simultaneous electrochemical determination of ascorbic acid, dopamine and uric acid. Anal Methods 5:3591. https://doi.org/10.1039/c3ay40572a
33. Li Z-F, Zhang H, Liu Q et al (2013) Fabrication of high-surface-area graphene/polyaniline nanocomposites and their application in supercapacitors. ACS Appl Mater Interfaces 5:2685–2691. https://doi.org/10.1021/am4001634
34. Cui F, Zhang X (2012) Electrochemical sensor for epinephrine based on a glassy carbon electrode modified with graphene/gold nanocomposites. J Electroanal Chem 669:35–41. https://doi.org/10.1016/j.jelechem.2012.01.021
35. Liu H, Chen X, Huang L et al (2014) Palladium nanoparticles embedded into graphene nanosheets: preparation, characterization, and nonenzymatic electrochemical detection of H 2 O 2. Electroanalysis 26:556–564. https://doi.org/10.1002/elan.201300428
36. Rakhi RB, Chen W, Cha D, Alshareef HN (2011) High performance supercapacitors using metal oxide anchored graphene nanosheet electrodes. J Mater Chem 21:16197. https://doi.org/10.1039/c1jm12963e
37. Li M, Tang Z, Leng M, Xue J (2014) Flexible solid-state supercapacitor based on graphene-based hybrid films. Adv Funct Mater 24:7495–7502. https://doi.org/10.1002/adfm.201402442
38. Fu K, Wang Y, Mao L et al (2016) Facile one-pot synthesis of graphene-porous carbon nanofibers hybrid support for Pt nanoparticles with high activity towards oxygen reduction. Electrochim Acta 215:427–434. https://doi.org/10.1016/j.electacta.2016.08.111
39. Nardecchia S, Carriazo D, Ferrer ML et al (2013) Three dimensional macroporous architectures and aerogels built of carbon nanotubes and/or graphene: synthesis and applications. Chem Soc Rev 42:794–830. https://doi.org/10.1039/C2CS35353A
40. Li C, Zhang X, Wang K et al (2015) Three dimensional graphene networks for supercapacitor electrode materials. New Carbon Mater 30:193–206. https://doi.org/10.1016/S1872-5805(15)60185-8
41. Song Y-Y, Zhang D, Gao W, Xia X-H (2005) Nonenzymatic glucose detection by using a three-dimensionally ordered, macroporous platinum template. Chem Eur J 11:2177–2182. https://doi.org/10.1002/chem.200400981
42. Niu X, Lan M, Zhao H, Chen C (2013) Highly sensitive and selective nonenzymatic detection of glucose using three-dimensional porous nickel nanostructures. Anal Chem 85:3561–3569. https://doi.org/10.1021/ac3030976
43. Wang D-W, Li F, Liu M et al (2008) 3D aperiodic hierarchical porous graphitic carbon material for high-rate electrochemical capacitive energy storage. Angew Chemie Int Ed 47:373–376. https://doi.org/10.1002/anie.200702721
44. Li J, Cassell A, Delzeit L et al (2002) Novel three-dimensional electrodes: electrochemical properties of carbon nanotube ensembles. J Phys Chem B 106:9299–9305. https://doi.org/10.1021/jp021201n
45. Wang L, Zhang Y, Yu J et al (2017) A green and simple strategy to prepare graphene foam-like three-dimensional porous carbon/Ni nanoparticles for glucose sensing. Sensors Actuators B Chem 239:172–179. https://doi.org/10.1016/j.snb.2016.06.173
46. Varley TS, Hirani M, Harrison G, Holt KB (2014) Nanodiamond surface redox chemistry: influence of physicochemical properties on catalytic processes. Faraday Discuss 172:349–364. https://doi.org/10.1039/C4FD00041B
47. Qin D, Gao S, Wang L et al (2017) Three-dimensional carbon nanofiber derived from bacterial cellulose for use in a Nafion matrix on a glassy carbon electrode for simultaneous voltammetric determination of trace levels of Cd(II) and Pb(II). Microchim Acta 184:2759–2766. https://doi.org/10.1007/s00604-017-2260-x
48. Huang D, Li X, Wang S et al (2017) Three-dimensional chemically reduced graphene oxide templated by silica spheres for

ammonia sensing. Sensors Actuators B Chem 252:956–964. https://doi.org/10.1016/j.snb.2017.05.117
49. Yong Y-C, Dong X-C, Chan-Park MB et al (2012) Macroporous and monolithic anode based on polyaniline hybridized three-dimensional graphene for high-performance microbial fuel cells. ACS Nano 6:2394–2400. https://doi.org/10.1021/nn204656d
50. Prasad KP, Chen Y, Chen P (2014) Three-dimensional graphene-carbon nanotube hybrid for high-performance enzymatic biofuel cells. ACS Appl Mater Interfaces 6:3387–3393. https://doi.org/10.1021/am405432b
51. Wu Z-S, Sun Y, Tan Y-Z et al (2012) Three-dimensional graphene-based macro- and mesoporous frameworks for high-performance electrochemical capacitive energy storage. J Am Chem Soc 134:19532–19535. https://doi.org/10.1021/ja308676h
52. Paek S, Yoo E, Honma I (2009) Enhanced cyclic performance and lithium storage capacity of SnO 2 /Graphene nanoporous electrodes with three-dimensionally delaminated flexible structure. Nano Lett 9:72–75. https://doi.org/10.1021/nl802484w
53. Zhang Y, Chu M, Yang L et al (2014) Three-dimensional graphene networks as a new substrate for immobilization of laccase and dopamine and its application in glucose/O 2 biofuel cell. ACS Appl Mater Interfaces 6:12808–12814. https://doi.org/10.1021/am502791h
54. Luo J, Liu J, Zeng Z et al (2013) Three-dimensional graphene foam supported Fe 3 O 4 lithium battery anodes with long cycle life and high rate capability. Nano Lett 13:6136–6143. https://doi.org/10.1021/nl403461n
55. Lee SH, Kim HW, Hwang JO et al (2010) Three-dimensional self-assembly of graphene oxide platelets into mechanically flexible macroporous carbon films. Angew Chemie Int Ed 49:10084–10088. https://doi.org/10.1002/anie.201006240
56. Xu Y, Lin Z, Huang X et al (2013) Flexible solid-state supercapacitors based on three-dimensional graphene hydrogel films. ACS Nano 7:4042–4049. https://doi.org/10.1021/nn4000836
57. Cao X, Shi Y, Shi W et al (2013) Preparation of MoS 2 -coated three-dimensional graphene networks for high-performance anode material in lithium-ion batteries. Small 9:3433–3438. https://doi.org/10.1002/smll.201202697
58. Ito Y, Tanabe Y, Sugawara K et al (2017) Three-dimensional porous graphene networks expand graphene-based electronic device applications. Phys Chem Chem Phys. https://doi.org/10.1039/C7CP07667C
59. Yang Y, Kang M, Fang S et al (2015) Electrochemical biosensor based on three-dimensional reduced graphene oxide and polyaniline nanocomposite for selective detection of mercury ions. Sensors Actuators B Chem 214:63–69. https://doi.org/10.1016/j.snb.2015.02.127
60. Dong X, Cao Y, Wang J et al (2012) Hybrid structure of zinc oxide nanorods and three dimensional graphene foam for supercapacitor and electrochemical sensor applications. RSC Adv 2:4364. https://doi.org/10.1039/c2ra01295b
61. Fang Q, Shen Y, Chen B (2015) Synthesis, decoration and properties of three-dimensional graphene-based macrostructures: a review. Chem Eng J 264:753–771. https://doi.org/10.1016/j.cej.2014.12.001
62. Xia XH, Chao DL, Zhang YQ et al (2014) Three-dimensional graphene and their integrated electrodes. Nano Today 9:785–807. https://doi.org/10.1016/j.nantod.2014.12.001
63. Sherrell PC, Mattevi C (2016) Mesoscale design of multifunctional 3D graphene networks. Mater Today 19:428–436. https://doi.org/10.1016/j.mattod.2015.12.004
64. Xi F, Zhao D, Wang X, Chen P (2013) Non-enzymatic detection of hydrogen peroxide using a functionalized three-dimensional graphene electrode. Electrochem Commun 26:81–84. https://doi.org/10.1016/j.elecom.2012.10.017
65. Cao X, Shi Y, Shi W et al (2011) Preparation of novel 3D graphene networks for supercapacitor applications. Small 7:3163–3168. https://doi.org/10.1002/smll.201100990
66. Chen Z, Ren W, Gao L et al (2011) Three-dimensional flexible and conductive interconnected graphene networks grown by chemical vapour deposition. Nat Mater 10:424–428. https://doi.org/10.1038/nmat3001
67. Cao X, Zeng Z, Shi W et al (2013) Three-Dimensional Graphene Network Composites for Detection of Hydrogen Peroxide. Small 9:1703–1707. https://doi.org/10.1002/smll.201200683
68. Dong X, Wang X, Wang L et al (2012) 3D graphene foam as a monolithic and macroporous carbon electrode for electrochemical sensing. ACS Appl Mater Interfaces 4:3129–3133. https://doi.org/10.1021/am300459m
69. Di Bernardo I, Avvisati G, Chen C et al (2018) Topology and doping effects in three-dimensional nanoporous graphene. Carbon N Y 131:258–265. https://doi.org/10.1016/j.carbon.2018.01.076
70. Wang X, Zhang Y, Zhi C et al (2013) Three-dimensional strutted graphene grown by substrate-free sugar blowing for high-power-density supercapacitors. Nat Commun 4:1–8. https://doi.org/10.1038/ncomms3905
71. Yuan M, Liu A, Zhao M et al (2014) Bimetallic PdCu nanoparticle decorated three-dimensional graphene hydrogel for non-enzymatic amperometric glucose sensor. Sensors Actuators B Chem 190:707–714. https://doi.org/10.1016/j.snb.2013.09.054
72. Xu Y, Sheng K, Li C, Shi G (2010) Self-assembled graphene hydrogel via a one-step hydrothermal process. ACS Nano 4:4324–4330. https://doi.org/10.1021/nn101187z
73. Chen P, Yang J-J, Li S-S et al (2013) Hydrothermal synthesis of macroscopic nitrogen-doped graphene hydrogels for ultrafast supercapacitor. Nano Energy 2:249–256. https://doi.org/10.1016/j.nanoen.2012.09.003
74. Xiao X, Roberts ME, Wheeler DR et al (2010) Increased mass transport at lithographically defined 3-D porous carbon electrodes. ACS Appl Mater Interfaces 2:3179–3184. https://doi.org/10.1021/am1006595
75. Xiao X, Beechem T, Wheeler DR et al (2014) Lithographically defined porous Ni–carbon nanocomposite supercapacitors. Nano 6:2629–2633. https://doi.org/10.1039/C3NR05751H
76. Xiao X, Beechem TE, Brumbach MT et al (2012) Lithographically defined three-dimensional graphene structures. ACS Nano 6:3573–3579. https://doi.org/10.1021/nn300655c
77. Byeon JH, Park D, Kim JY (2015) An aerosol-based soft lithography to fabricate nanoscale silver dots and rings for spectroscopic applications. Nano 7:2271–2275. https://doi.org/10.1039/C4NR07476A
78. Liu F, Piao Y, Choi JS, Seo TS (2013) Three-dimensional graphene micropillar based electrochemical sensor for phenol detection. Biosens Bioelectron 50:387–392. https://doi.org/10.1016/j.bios.2013.06.055
79. Sun G, Lu J, Ge S et al (2013) Ultrasensitive electrochemical immunoassay for carcinoembryonic antigen based on three-dimensional macroporous gold nanoparticles/graphene composite platform and multienzyme functionalized nanoporous silver label. Anal Chim Acta 775:85–92. https://doi.org/10.1016/j.aca.2013.03.009
80. Choi BG, Yang M, Hong WH et al (2012) 3D macroporous graphene frameworks for supercapacitors with high energy and power densities. ACS Nano 6:4020–4028. https://doi.org/10.1021/nn3003345
81. Shao Q, Tang J, Lin Y et al (2013) Synthesis and characterization of graphene hollow spheres for application in supercapacitors. J Mater Chem A 1:15423. https://doi.org/10.1039/c3ta12789c
82. Yu B, Kuang D, Liu S et al (2014) Template-assisted self-assembly method to prepare three-dimensional reduced graphene oxide

for dopamine sensing. Sensors Actuators B Chem 205:120–126. https://doi.org/10.1016/j.snb.2014.08.038
83. Luo J, Ma Q, Gu H et al (2015) Three-dimensional graphene-polyaniline hybrid hollow spheres by layer-by-layer assembly for application in supercapacitor. Electrochim Acta 173:184–192. https://doi.org/10.1016/j.electacta.2015.05.053
84. Gao W (2015) The chemistry of graphene oxide. graphene oxide. Springer International Publishing, Cham, pp 61–95
85. Sheng K, Sun Y, Li C et al (2012) Ultrahigh-rate supercapacitors based on eletrochemically reduced graphene oxide for ac line-filtering. Sci Rep 2:247. https://doi.org/10.1038/srep00247
86. Chen K, Chen L, Chen Y et al (2012) Three-dimensional porous graphene-based composite materials: electrochemical synthesis and application. J Mater Chem 22:20968. https://doi.org/10.1039/c2jm34816k
87. Shi F, Xi J, Hou F et al (2016) Application of three-dimensional reduced graphene oxide-gold composite modified electrode for direct electrochemistry and electrocatalysis of myoglobin. Mater Sci Eng C 58:450–457. https://doi.org/10.1016/j.msec.2015.08.049
88. Cui M, Xu B, Hu C et al (2013) Direct electrochemistry and electrocatalysis of glucose oxidase on three-dimensional interpenetrating, porous graphene modified electrode. Electrochim Acta 98:48–53. https://doi.org/10.1016/j.electacta.2013.03.040
89. Sun W, Hou F, Gong S et al (2015) Direct electrochemistry and electrocatalysis of hemoglobin on three-dimensional graphene modified carbon ionic liquid electrode. Sensors Actuators B Chem 219:331–337. https://doi.org/10.1016/j.snb.2015.05.015
90. Zhu C, Han TY-J, Duoss EB et al (2015) Highly compressible 3D periodic graphene aerogel microlattices. Nat Commun 6:6962. https://doi.org/10.1038/ncomms7962
91. Jeon MS, Jeon Y, Hwang JH et al (2018) Fabrication of three-dimensional porous carbon scaffolds with tunable pore sizes for effective cell confinement. Carbon N Y 130:814–821. https://doi.org/10.1016/j.carbon.2018.01.050
92. Shi Q, Cha Y, Song Y et al (2016) 3D graphene-based hybrid materials: synthesis and applications in energy storage and conversion. Nano 8:15414–15447. https://doi.org/10.1039/C6NR04770J
93. Zhang R, Cao Y, Li P et al (2014) Three-dimensional porous graphene sponges assembled with the combination of surfactant and freeze-drying. Nano Res 7:1477–1487. https://doi.org/10.1007/s12274-014-0508-x
94. Lu L, Guo L, Kang T, Cheng S (2017) A gold electrode modified with a three-dimensional graphene-DNA composite for sensitive voltammetric determination of dopamine. Microchim Acta 184:2949–2957. https://doi.org/10.1007/s00604-017-2267-3
95. Wang G, Wang B, Wang X et al (2009) Sn/graphene nanocomposite with 3D architecture for enhanced reversible lithium storage in lithium ion batteries. J Mater Chem 19:8378. https://doi.org/10.1039/b914650d
96. Liu L, Feng T, Wang C et al (2014) Magnetic three-dimensional graphene nanoparticles for the preconcentration of endocrine-disrupting phenols. Microchim Acta 181:1249–1255. https://doi.org/10.1007/s00604-014-1234-5
97. Amiri A, Ghaemi F (2017) Microextraction in packed syringe by using a three-dimensional carbon nanotube/carbon nanofiber–graphene nanostructure coupled to dispersive liquid-liquid microextraction for the determination of phthalate esters in water samples. Microchim Acta 184:3851–3858. https://doi.org/10.1007/s00604-017-2416-8
98. Chen Z, Li H, Tian R et al (2016) Three dimensional graphene aerogels as binder-less, freestanding, elastic and high-performance electrodes for lithium-ion batteries. Sci Rep 6:27365. https://doi.org/10.1038/srep27365
99. Chen M, Hou C, Huo D et al (2017) A sensitive electrochemical DNA biosensor based on three-dimensional nitrogen-doped graphene and Fe 3 O 4 nanoparticles. Sensors Actuators B Chem 239:421–429. https://doi.org/10.1016/j.snb.2016.08.036
100. Baig N, Sajid M (2017) Applications of layered double hydroxides based electrochemical sensors for determination of environmental pollutants: a review. Trends Environ Anal Chem 16:1–15. https://doi.org/10.1016/j.teac.2017.10.003
101. Yu X, Lu B, Xu Z (2014) Super long-life supercapacitors based on the construction of nanohoneycomb-like strongly coupled CoMoO 4 -3D graphene hybrid electrodes. Adv Mater 26:1044–1051. https://doi.org/10.1002/adma.201304148
102. Baig N, Kawde A-N (2016) A cost-effective disposable graphene-modified electrode decorated with alternating layers of Au NPs for the simultaneous detection of dopamine and uric acid in human urine. RSC Adv 6:80756–80765. https://doi.org/10.1039/C6RA10055D
103. Yu X, Sheng K, Shi G (2014) A three-dimensional interpenetrating electrode of reduced graphene oxide for selective detection of dopamine. Analyst 139:4525–4531. https://doi.org/10.1039/C4AN00604F
104. Ruiyi L, Haiyan Z, Zaijun L, Junkang L (2018) Electrochemical determination of acetaminophen using a glassy carbon electrode modified with a hybrid material consisting of graphene aerogel and octadecylamine-functionalized carbon quantum dots. Microchim Acta 185:145. https://doi.org/10.1007/s00604-018-2688-7
105. Gao X, Yue H, Song S et al (2018) 3-Dimensional hollow graphene balls for voltammetric sensing of levodopa in the presence of uric acid. Microchim Acta 185:91. https://doi.org/10.1007/s00604-017-2644-y
106. Zhang X, Ju H, Wang J, Zhang X (2008) Nitric oxide (NO) electrochemical sensors. Electrochem. Sensors, Biosens. their Biomed. Appl. Elsevier, pp 1–29
107. Ng SR, Guo CX, Li CM (2011) Highly sensitive nitric oxide sensing using three-dimensional graphene/ionic liquid nanocomposite. Electroanalysis 23:442–448. https://doi.org/10.1002/elan.201000344
108. Kawde A-N, Aziz MA, El-Zohri M et al (2017) Cathodized gold nanoparticle-modified graphite pencil electrode for non-enzymatic sensitive voltammetric detection of glucose. Electroanalysis 29:1214–1221. https://doi.org/10.1002/elan.201600709
109. Kawde A-N, Aziz M, Baig N, Temerk Y (2015) A facile fabrication of platinum nanoparticle-modified graphite pencil electrode for highly sensitive detection of hydrogen peroxide. J Electroanal Chem 740:68–74. https://doi.org/10.1016/j.jelechem.2015.01.005
110. Yuan Y, Zheng Y, Liu J et al (2017) Non-enzymatic amperometric hydrogen peroxide sensor using a glassy carbon electrode modified with gold nanoparticles deposited on CVD-grown graphene. Microchim Acta 184:4723–4729. https://doi.org/10.1007/s00604-017-2499-2
111. Wang L, Qin K, Li J et al (2018) Doping and controllable pore size enhanced electrochemical performance of free-standing 3D graphene films. Appl Surf Sci 427:598–604. https://doi.org/10.1016/j.apsusc.2017.08.204
112. Zhu Q, Bao J, Huo D et al (2017) 3D Graphene hydrogel – gold nanoparticles nanocomposite modified glassy carbon electrode for the simultaneous determination of ascorbic acid, dopamine and uric acid. Sensors Actuators B Chem 238:1316–1323. https://doi.org/10.1016/J.SNB.2016.09.116
113. Kung C-C, Lin P-Y, Buse FJ et al (2014) Preparation and characterization of three dimensional graphene foam supported platinum–ruthenium bimetallic nanocatalysts for hydrogen peroxide based electrochemical biosensors. Biosens Bioelectron 52:1–7. https://doi.org/10.1016/j.bios.2013.08.025

114. Maiyalagan T, Dong X, Chen P, Wang X (2012) Electrodeposited Pt on three-dimensional interconnected graphene as a free-standing electrode for fuel cell application. J Mater Chem 22: 5286. https://doi.org/10.1039/c2jm16541d
115. Dechtrirat D, Sookcharoenpinyo B, Prajongtat P et al (2018) An electrochemical MIP sensor for selective detection of salbutamol based on a graphene/PEDOT:PSS modified screen printed carbon electrode. RSC Adv 8:206–212. https://doi.org/10.1039/C7RA09601A
116. Mazloum-Ardakani M, Barazesh B, Khoshroo A et al (2018) A new composite consisting of electrosynthesized conducting polymers, graphene sheets and biosynthesized gold nanoparticles for biosensing acute lymphoblastic leukemia. Bioelectrochemistry 121:38–45. https://doi.org/10.1016/j.bioelechem.2017.12.010
117. Wang M-H, Ji B-W, Gu X-W et al (2018) Direct electrodeposition of graphene enhanced conductive polymer on microelectrode for biosensing application. Biosens Bioelectron 99:99–107. https://doi.org/10.1016/j.bios.2017.07.030
118. Lei W, Si W, Xu Y et al (2014) Conducting polymer composites with graphene for use in chemical sensors and biosensors. Microchim Acta 181:707–722. https://doi.org/10.1007/s00604-014-1160-6
119. Tanaka Y, Oda S, Yamaguchi H et al (2007) 15 N− 15 N J -coupling across Hg II : direct observation of Hg II -mediated T −T base pairs in a DNA duplex. J Am Chem Soc 129:244–245. https://doi.org/10.1021/ja065552h
120. Peng DL, Ji HF, Dong XD et al (2016) Highly sensitive electrochemical bioassay for Hg(II) detection based on plasma-polymerized propargylamine and three-dimensional reduced graphene oxide nanocomposite. Plasma Chem Plasma Process 36:1051–1065. https://doi.org/10.1007/s11090-016-9707-4
121. Liu J, Wang J, Wang T et al (2015) Three-dimensional electrochemical immunosensor for sensitive detection of carcinoembryonic antigen based on monolithic and macroporous graphene foam. Biosens Bioelectron 65:281–286. https://doi.org/10.1016/j.bios.2014.10.016
122. Cheng Q, Tang J, Ma J et al (2011) Graphene and carbon nanotube composite electrodes for supercapacitors with ultra-high energy density. Phys Chem Chem Phys 13:17615. https://doi.org/10.1039/c1cp21910c
123. Liu J, Wang X, Wang T et al (2014) Functionalization of monolithic and porous three-dimensional graphene by one-step chitosan electrodeposition for enzymatic biosensor. ACS Appl Mater Interfaces 6:19997–20002. https://doi.org/10.1021/am505547f
124. Fernandes R, Wu L-Q, Chen T et al (2003) Electrochemically induced deposition of a polysaccharide hydrogel onto a patterned surface. Langmuir 19:4058–4062. https://doi.org/10.1021/la027052h
125. Luo X-L, Xu J-J, Du Y, Chen H-Y (2004) A glucose biosensor based on chitosan–glucose oxidase–gold nanoparticles biocomposite formed by one-step electrodeposition. Anal Biochem 334:284–289. https://doi.org/10.1016/j.ab.2004.07.005
126. Maaoui H, Singh SK, Teodorescu F et al (2017) Copper oxide supported on three-dimensional ammonia-doped porous reduced graphene oxide prepared through electrophoretic deposition for non-enzymatic glucose sensing. Electrochim Acta 224:346–354. https://doi.org/10.1016/j.electacta.2016.12.078
127. Tian Y, Wei Z, Zhang K et al (2017) Three-dimensional phosphorus-doped graphene as an efficient metal-free electrocatalyst for electrochemical sensing. Sensors Actuators B Chem 241:584–591. https://doi.org/10.1016/j.snb.2016.10.113
128. Xu J, Wang Y, Hu S (2017) Nanocomposites of graphene and graphene oxides: synthesis, molecular functionalization and application in electrochemical sensors and biosensors. A review. Microchim Acta 184:1–44. https://doi.org/10.1007/s00604-016-2007-0
129. Chen M, Su H, Mao L et al (2018) Highly sensitive electrochemical DNA sensor based on the use of three-dimensional nitrogen-doped graphene. Microchim Acta 185:51. https://doi.org/10.1007/s00604-017-2588-2
130. Mazaheri M, Aashuri H, Simchi A (2017) Three-dimensional hybrid graphene/nickel electrodes on zinc oxide nanorod arrays as non-enzymatic glucose biosensors. Sensors Actuators B Chem 251:462–471. https://doi.org/10.1016/j.snb.2017.05.062
131. Kim B-J, Yang G, Joo Park M et al (2013) Three-dimensional graphene foam-based transparent conductive electrodes in GaN-based blue light-emitting diodes. Appl Phys Lett 102:161902. https://doi.org/10.1063/1.4801763
132. Lv W, Tao Y, Ni W et al (2011) One-pot self-assembly of three-dimensional graphene macroassemblies with porous core and layered shell. J Mater Chem 21:12352. https://doi.org/10.1039/c1jm11728a
133. Jiang X, Ma Y, Li J et al (2010) Self-assembly of reduced graphene oxide into three-dimensional architecture by divalent ion linkage. J Phys Chem C 114:22462–22465. https://doi.org/10.1021/jp108081g
134. Stankovich S, Dikin DA, Piner RD et al (2007) Synthesis of graphene-based nanosheets via chemical reduction of exfoliated graphite oxide. Carbon N Y 45:1558–1565. https://doi.org/10.1016/j.carbon.2007.02.034
135. Shao Y, Wang J, Engelhard M et al (2010) Facile and controllable electrochemical reduction of graphene oxide and its applications. J Mater Chem 20:743–748. https://doi.org/10.1039/B917975E
136. Erickson K, Erni R, Lee Z et al (2010) Determination of the local chemical structure of graphene oxide and reduced graphene oxide. Adv Mater 22:4467–4472. https://doi.org/10.1002/adma.201000732
137. Li N, Zhang Q, Gao S et al (2013) Three-dimensional graphene foam as a biocompatible and conductive scaffold for neural stem cells. Sci Rep 3:1604. https://doi.org/10.1038/srep01604
138. Dong X, Wang J, Wang J et al (2012) Supercapacitor electrode based on three-dimensional graphene–polyaniline hybrid. Mater Chem Phys 134:576–580. https://doi.org/10.1016/j.matchemphys.2012.03.066
139. Yang Z, Yan C, Liu J et al (2015) Designing 3D graphene networks via a 3D-printed Ni template. RSC Adv 5:29397–29400. https://doi.org/10.1039/C5RA03454J
140. Yang Z, Chabi S, Xia Y, Zhu Y (2015) Preparation of 3D graphene-based architectures and their applications in supercapacitors. Prog Nat Sci Mater Int 25:554–562. https://doi.org/10.1016/j.pnsc.2015.11.010